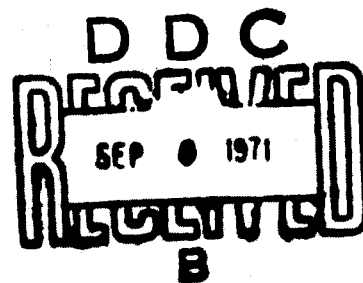


AD 729257

NORTHROP CORPORATE LABORATORIES

**CARBON MONOXIDE LASER STUDIES
FINAL REPORT: PART I
AUGUST 1971**

Prepared by
M. L. Bhaumik
Northrop Corporate Laboratories



Office of Naval Research
Contract No. N00014-71-G-0037
1 August 1970 through 31 July 1971

Sponsored by
Advanced Research Projects Agency
Order No. 306

NATIONAL TECHNICAL
INFORMATION SERVICE

STATEMENT A
For public release
Distribution unlimited

NOTICE

The views and conclusions contained in this document are those of the authors and should not be interpreted as necessarily representing the official policies, either expressed or implied, of the Advanced Research Projects Agency or the U. S. Government.

CLASSIFICATION	GROUP 1	GROUP 2	GROUP 3
GROUP 1	<input checked="" type="checkbox"/>	<input type="checkbox"/>	<input type="checkbox"/>
GROUP 2	<input type="checkbox"/>	<input type="checkbox"/>	<input type="checkbox"/>
GROUP 3	<input type="checkbox"/>	<input type="checkbox"/>	<input type="checkbox"/>
GROUP 4	<input type="checkbox"/>	<input type="checkbox"/>	<input type="checkbox"/>
GROUP 5	<input type="checkbox"/>	<input type="checkbox"/>	<input type="checkbox"/>
GROUP 6	<input type="checkbox"/>	<input type="checkbox"/>	<input type="checkbox"/>
GROUP 7	<input type="checkbox"/>	<input type="checkbox"/>	<input type="checkbox"/>
GROUP 8	<input type="checkbox"/>	<input type="checkbox"/>	<input type="checkbox"/>
GROUP 9	<input type="checkbox"/>	<input type="checkbox"/>	<input type="checkbox"/>
GROUP 10	<input type="checkbox"/>	<input type="checkbox"/>	<input type="checkbox"/>
GROUP 11	<input type="checkbox"/>	<input type="checkbox"/>	<input type="checkbox"/>
GROUP 12	<input type="checkbox"/>	<input type="checkbox"/>	<input type="checkbox"/>
GROUP 13	<input type="checkbox"/>	<input type="checkbox"/>	<input type="checkbox"/>
GROUP 14	<input type="checkbox"/>	<input type="checkbox"/>	<input type="checkbox"/>
GROUP 15	<input type="checkbox"/>	<input type="checkbox"/>	<input type="checkbox"/>
GROUP 16	<input type="checkbox"/>	<input type="checkbox"/>	<input type="checkbox"/>
GROUP 17	<input type="checkbox"/>	<input type="checkbox"/>	<input type="checkbox"/>
GROUP 18	<input type="checkbox"/>	<input type="checkbox"/>	<input type="checkbox"/>
GROUP 19	<input type="checkbox"/>	<input type="checkbox"/>	<input type="checkbox"/>
GROUP 20	<input type="checkbox"/>	<input type="checkbox"/>	<input type="checkbox"/>
GROUP 21	<input type="checkbox"/>	<input type="checkbox"/>	<input type="checkbox"/>
GROUP 22	<input type="checkbox"/>	<input type="checkbox"/>	<input type="checkbox"/>
GROUP 23	<input type="checkbox"/>	<input type="checkbox"/>	<input type="checkbox"/>
GROUP 24	<input type="checkbox"/>	<input type="checkbox"/>	<input type="checkbox"/>
GROUP 25	<input type="checkbox"/>	<input type="checkbox"/>	<input type="checkbox"/>
GROUP 26	<input type="checkbox"/>	<input type="checkbox"/>	<input type="checkbox"/>
GROUP 27	<input type="checkbox"/>	<input type="checkbox"/>	<input type="checkbox"/>
GROUP 28	<input type="checkbox"/>	<input type="checkbox"/>	<input type="checkbox"/>
GROUP 29	<input type="checkbox"/>	<input type="checkbox"/>	<input type="checkbox"/>
GROUP 30	<input type="checkbox"/>	<input type="checkbox"/>	<input type="checkbox"/>
GROUP 31	<input type="checkbox"/>	<input type="checkbox"/>	<input type="checkbox"/>
GROUP 32	<input type="checkbox"/>	<input type="checkbox"/>	<input type="checkbox"/>
GROUP 33	<input type="checkbox"/>	<input type="checkbox"/>	<input type="checkbox"/>
GROUP 34	<input type="checkbox"/>	<input type="checkbox"/>	<input type="checkbox"/>
GROUP 35	<input type="checkbox"/>	<input type="checkbox"/>	<input type="checkbox"/>
GROUP 36	<input type="checkbox"/>	<input type="checkbox"/>	<input type="checkbox"/>
GROUP 37	<input type="checkbox"/>	<input type="checkbox"/>	<input type="checkbox"/>
GROUP 38	<input type="checkbox"/>	<input type="checkbox"/>	<input type="checkbox"/>
GROUP 39	<input type="checkbox"/>	<input type="checkbox"/>	<input type="checkbox"/>
GROUP 40	<input type="checkbox"/>	<input type="checkbox"/>	<input type="checkbox"/>
GROUP 41	<input type="checkbox"/>	<input type="checkbox"/>	<input type="checkbox"/>
GROUP 42	<input type="checkbox"/>	<input type="checkbox"/>	<input type="checkbox"/>
GROUP 43	<input type="checkbox"/>	<input type="checkbox"/>	<input type="checkbox"/>
GROUP 44	<input type="checkbox"/>	<input type="checkbox"/>	<input type="checkbox"/>
GROUP 45	<input type="checkbox"/>	<input type="checkbox"/>	<input type="checkbox"/>
GROUP 46	<input type="checkbox"/>	<input type="checkbox"/>	<input type="checkbox"/>
GROUP 47	<input type="checkbox"/>	<input type="checkbox"/>	<input type="checkbox"/>
GROUP 48	<input type="checkbox"/>	<input type="checkbox"/>	<input type="checkbox"/>
GROUP 49	<input type="checkbox"/>	<input type="checkbox"/>	<input type="checkbox"/>
GROUP 50	<input type="checkbox"/>	<input type="checkbox"/>	<input type="checkbox"/>
GROUP 51	<input type="checkbox"/>	<input type="checkbox"/>	<input type="checkbox"/>
GROUP 52	<input type="checkbox"/>	<input type="checkbox"/>	<input type="checkbox"/>
GROUP 53	<input type="checkbox"/>	<input type="checkbox"/>	<input type="checkbox"/>
GROUP 54	<input type="checkbox"/>	<input type="checkbox"/>	<input type="checkbox"/>
GROUP 55	<input type="checkbox"/>	<input type="checkbox"/>	<input type="checkbox"/>
GROUP 56	<input type="checkbox"/>	<input type="checkbox"/>	<input type="checkbox"/>
GROUP 57	<input type="checkbox"/>	<input type="checkbox"/>	<input type="checkbox"/>
GROUP 58	<input type="checkbox"/>	<input type="checkbox"/>	<input type="checkbox"/>
GROUP 59	<input type="checkbox"/>	<input type="checkbox"/>	<input type="checkbox"/>
GROUP 60	<input type="checkbox"/>	<input type="checkbox"/>	<input type="checkbox"/>
GROUP 61	<input type="checkbox"/>	<input type="checkbox"/>	<input type="checkbox"/>
GROUP 62	<input type="checkbox"/>	<input type="checkbox"/>	<input type="checkbox"/>
GROUP 63	<input type="checkbox"/>	<input type="checkbox"/>	<input type="checkbox"/>
GROUP 64	<input type="checkbox"/>	<input type="checkbox"/>	<input type="checkbox"/>
GROUP 65	<input type="checkbox"/>	<input type="checkbox"/>	<input type="checkbox"/>
GROUP 66	<input type="checkbox"/>	<input type="checkbox"/>	<input type="checkbox"/>
GROUP 67	<input type="checkbox"/>	<input type="checkbox"/>	<input type="checkbox"/>
GROUP 68	<input type="checkbox"/>	<input type="checkbox"/>	<input type="checkbox"/>
GROUP 69	<input type="checkbox"/>	<input type="checkbox"/>	<input type="checkbox"/>
GROUP 70	<input type="checkbox"/>	<input type="checkbox"/>	<input type="checkbox"/>
GROUP 71	<input type="checkbox"/>	<input type="checkbox"/>	<input type="checkbox"/>
GROUP 72	<input type="checkbox"/>	<input type="checkbox"/>	<input type="checkbox"/>
GROUP 73	<input type="checkbox"/>	<input type="checkbox"/>	<input type="checkbox"/>
GROUP 74	<input type="checkbox"/>	<input type="checkbox"/>	<input type="checkbox"/>
GROUP 75	<input type="checkbox"/>	<input type="checkbox"/>	<input type="checkbox"/>
GROUP 76	<input type="checkbox"/>	<input type="checkbox"/>	<input type="checkbox"/>
GROUP 77	<input type="checkbox"/>	<input type="checkbox"/>	<input type="checkbox"/>
GROUP 78	<input type="checkbox"/>	<input type="checkbox"/>	<input type="checkbox"/>
GROUP 79	<input type="checkbox"/>	<input type="checkbox"/>	<input type="checkbox"/>
GROUP 80	<input type="checkbox"/>	<input type="checkbox"/>	<input type="checkbox"/>
GROUP 81	<input type="checkbox"/>	<input type="checkbox"/>	<input type="checkbox"/>
GROUP 82	<input type="checkbox"/>	<input type="checkbox"/>	<input type="checkbox"/>
GROUP 83	<input type="checkbox"/>	<input type="checkbox"/>	<input type="checkbox"/>
GROUP 84	<input type="checkbox"/>	<input type="checkbox"/>	<input type="checkbox"/>
GROUP 85	<input type="checkbox"/>	<input type="checkbox"/>	<input type="checkbox"/>
GROUP 86	<input type="checkbox"/>	<input type="checkbox"/>	<input type="checkbox"/>
GROUP 87	<input type="checkbox"/>	<input type="checkbox"/>	<input type="checkbox"/>
GROUP 88	<input type="checkbox"/>	<input type="checkbox"/>	<input type="checkbox"/>
GROUP 89	<input type="checkbox"/>	<input type="checkbox"/>	<input type="checkbox"/>
GROUP 90	<input type="checkbox"/>	<input type="checkbox"/>	<input type="checkbox"/>
GROUP 91	<input type="checkbox"/>	<input type="checkbox"/>	<input type="checkbox"/>
GROUP 92	<input type="checkbox"/>	<input type="checkbox"/>	<input type="checkbox"/>
GROUP 93	<input type="checkbox"/>	<input type="checkbox"/>	<input type="checkbox"/>
GROUP 94	<input type="checkbox"/>	<input type="checkbox"/>	<input type="checkbox"/>
GROUP 95	<input type="checkbox"/>	<input type="checkbox"/>	<input type="checkbox"/>
GROUP 96	<input type="checkbox"/>	<input type="checkbox"/>	<input type="checkbox"/>
GROUP 97	<input type="checkbox"/>	<input type="checkbox"/>	<input type="checkbox"/>
GROUP 98	<input type="checkbox"/>	<input type="checkbox"/>	<input type="checkbox"/>
GROUP 99	<input type="checkbox"/>	<input type="checkbox"/>	<input type="checkbox"/>
GROUP 100	<input type="checkbox"/>	<input type="checkbox"/>	<input type="checkbox"/>

1

DOCUMENT CONTROL DATA - R & D

Security classification of title, body of abstract and indexing annotation must be entered when the overall report is classified)

1. ORIGINATING ACTIVITY (Corporate author) NORTHROP CORPORATE LABORATORIES 3401 WEST BROADWAY HAWTHORNE, CALIFORNIA		2a. REPORT SECURITY CLASSIFICATION UNCLASSIFIED	
3. REPORT TITLE CARBON MONOXIDE LASER STUDIES - FINAL REPORT: PART I		2b. GROUP --	
4. DESCRIPTIVE NOTES (Type of report and inclusive dates) FINAL REPORT: PART I AUGUST 1971			
5. AUTHOR(S) (First name, middle initial, last name) BHAAUMIK, MANI L.			
6. REPORT DATE AUGUST 1971	7a. TOTAL NO. OF PAGES 51	7b. NO. OF REFS 15	
8a. CONTRACT OR GRANT NO Contract N00014-71-C-0037	9a. ORIGINATOR'S REPORT NUMBER(S) NCL 71-31R		
b. PROJECT NO ARPA Order No. 306	9b. OTHER REPORT NO(S) (Any other number that may be assigned this report) --		
c. --			
d. --			
10. DISTRIBUTION STATEMENT DISTRIBUTION OF THIS DOCUMENT IS UNLIMITED.			
11. SUPPLEMENTARY NOTES NONE		12. SPONSORING MILITARY ACTIVITY Office of Naval Research Department of the Navy Arlington, Virginia 22217	
13. ABSTRACT In an experimental and analytical study of carbon monoxide (CO) lasers, sponsored by the Advanced Research Project Agency under the Office of Naval Research Contract N00014-71-C-0037, the characteristics of the laser have been determined and the dominant mechanisms identified. The study shows that in an electrically excited CO laser, the population inversion occurs due to pumping of the lower vibrational levels by electron impact followed by anharmonic pumping to the upper lasing levels. (U) Overall efficiencies up to 47% have been achieved at 77°K. The small signal gains of the various vibrational rotational lines were measured. The populations of the lasing level were determined from these measurements to be 6% of the total number of CO molecules. The saturation parameter was estimated from the gain measurements to be 4w/cm ² at 125°K and 22 w/cm ² at 200°K. (U)			

14 KEY WORDS	LINK A		LINK B		LINK C	
	ROLE	WT	ROLE	WT	ROLE	WT
CO Laser Laser Gas Laser Basic Mechanisms Gain Coefficient Saturation Parameters High Laser Efficiency						

NCL 71-31R

**CARBON MONOXIDE LASER STUDIES
FINAL REPORT: PART I
AUGUST 1971**

**Office of Naval Research
Contract No. N00014-71-C-0037
1 August 1970 through 31 July 1971**

Prepared by

M. L. Bhaumik

**Sponsored by
Advanced Research Projects Agency
Order No. 306**

Principal Investigator:

Dr. M. L. Bhaumik

Tel: (213) 675-4611, Ext 4925

**NORTHROP CORPORATE LABORATORIES
3401 West Broadway
Hawthorne, California 90250**

TABLE OF CONTENTS

1.0	SUMMARY	1
2.0	INTRODUCTION	3
3.0	DISCUSSION OF THE CO MOLECULAR LASER	4
4.0	MEASUREMENT OF CO LASER OPERATING CHARACTERISTICS	9
5.0	THE ROLE OF VARIOUS GAS CONSTITUENTS	15
6.0	SPECTRAL MEASUREMENTS	18
	6.1 Measurement of Laser Output Spectra at Various Temperatures	18
	6.2 Observation of Anharmonic Pumping	26
	6.3 Time Resolved Spectroscopic Measurement of CO Laser	29
7.0	GAIN MEASUREMENT AND ANALYSIS	32
	7.1 Small Signal Gain Measurement	32
	7.2 Interpretation of Gain Measurements	34
	7.3 Measurement of Saturation Parameters	37
8.0	MEASUREMENT OF V-V RELAXATION RATE	45
9.0	CONCLUSION	48
10.0	REFERENCES	50

1.0 SUMMARY

This report describes the results of a study of the carbon monoxide laser undertaken at the Northrop Corporate Laboratories, between August 1, 1970 to July 31, 1971, supported by ARPA-ONR funds under Contract N00014-71-C-0037. The objective of this program was to conduct fundamental experimental and analytical studies in order to understand the basic mechanisms of the CO laser. The experimental measurements and analysis of this study are presented in this report. The theoretical modeling studies are presented in a separate companion report¹.

The operating characteristics of the CO laser have been measured and the roles of various ingredients necessary for an optimum gas composition have been determined. The high efficiency (47%) obtained with the CO laser has been explained in terms of the energy level schemes as well as the kinetics of the molecules and the electrons.

Extensive measurements of the laser output spectrum were made as a function of temperature. The manifestation of anharmonic pumping in the CO laser has been clearly demonstrated from the study of the temperature dependence of the spectra. A time-resolved spectroscopic study of the output spectrum was also performed. These results show that the presence of more than one rotational line in the laser spectrum is due to cascading as well as to the somewhat low rate of rotational cross-relaxation in CO.

The small signal gain measurements were also made both at room and liquid nitrogen temperatures. The population densities of the various lasing levels were determined from the gain coefficients. The population inversion at low temperatures is found to be of the same order of magnitude as that of CO₂ lasers. A value for the saturation intensity was determined for both the low and high intensity regions of the low pressure CO laser.

The rate of vibrational cross-relaxation was determined from a double Q-switching experiment. The results have been compared with those reported by others. Finally, conclusions regarding the mechanism of the CO laser as determined by the present study are presented along with a discussion of the potential of the CO laser.

2.0 INTRODUCTION

Currently, there is considerable interest in the development of molecular gas lasers capable of delivering high efficiency at high output powers in the infrared region. Of particular interest are the CO₂ and CO molecular lasers, because of their output wavelength in the atmospheric transmission windows near 10 and 5 micron wavelengths, respectively. While much work has been done on CO₂ lasers, the interest in the CO laser is more recent, and considerably fewer studies have been reported. The work reported here was undertaken to determine the operating characteristics of the laser and the mechanism of the laser operation.

The study of the spectral characteristics and the small signal gain coefficients are fundamental to the understanding of the basic mechanisms of the laser operation. Therefore, the bulk of the work was devoted to the measurement and analysis of these parameters. Considerable effort was also spent on the measurement and understanding of other basic parameters such as the efficiency, saturation parameter, etc., which are essential for the design of laser devices. Presentation of these experimental data is included in this report along with a detailed discussion of the CO molecular laser.

3.0 DISCUSSION OF THE CO MOLECULAR LASER

Molecular gas lasers have been unsurpassed for obtaining high efficiencies with high average power operation. For example, up to 30% has been realized for the CO₂ laser, and since this is basically a three-level system, the upper limit is the 40% quantum efficiency. However, diatomic molecular lasers such as CO offer significant advantages for obtaining operation at even higher efficiencies.

A diatomic molecule has only one ladder of energy levels, corresponding to a single vibrational mode (in contrast to CO₂, which has three different modes), and therefore it is possible to have a (nearly) 100% quantum efficiency. The reason for this is that the lower laser level of a given transition can serve as the upper level of a subsequent transition, thus permitting the vibrational energy to be extracted as coherent radiation through several pairs of levels for which the populations are sufficiently inverted. For CO, it should be noted that, as a result of rapid redistribution of vibrational energy among the levels, a molecule reaching a terminal laser level can be re-excited, and thus the absence of lasing on the lower levels need not limit the efficiency. This advantage is in contrast to the CO₂ system, for which the energy of the lower laser level is rapidly dissipated as heat energy through VT collisional relaxation.

Clearly, one very serious problem which exists for some diatomic molecules (e. g. , HF, HBr, NO) is the very fast vibration-translation (VT) collisional relaxation processes that cause the molecules to lose vibrational energy quickly as heat. Among the diatomic molecules which are useful for laser applications, CO is unique in that respect, since its VT lifetimes are relatively long: typically 2, 2×10^{-3} , and 10^3 atm. sec respectively for CO-CO, CO-He, and CO-Ar collisions for $v = 1 \rightarrow v = 0$ deactivation²⁻⁴.

(Of course, these time constants decrease for higher vibrational levels since the energies of the quanta decrease and the transition moments increase.) For a diatomic molecule, the ladder of vibrational levels has energy spacings which are nearly resonant except for the anharmonic defect, and thus, efficient vibrational cross-relaxation processes are possible. In fact, for the CO laser, it is these rapid near-resonant vibration-vibration exchange collisions (VV) that dominate the molecular kinetics and predominantly determine the structure of the vibrational population distribution. For the lower levels, the populations are typically quasi-Boltzmann, with insufficient partial inversions to produce positive laser gain on the lowest transitions. As Treanor⁵ and others have observed, this distribution will become non-Boltzmann at higher vibrational levels, due to the anharmonic VV pumping mechanism.

For the longitudinal electric discharge CO lasers investigated here, the primary process of pumping energy into the CO vibrational levels is by resonant inelastic electron scattering with the formation of compound states CO^- and N_2^- , which then decay into excited vibrational states. Cross-sections for these excitation processes have been experimentally measured by Schulz⁶, and this data together with knowledge of the electron distribution function makes it possible to calculate the electron pumping rates. If the electron energy distribution is assumed to be Boltzmann, with a temperature $T_e \sim 15,000^\circ\text{K}$ and electron density $n_e \sim 3 \times 10^9 \text{ cm}^{-3}$, these rates are typically about 51 sec^{-1} and 3.0 sec^{-1} , respectively, for excitation by electron-molecule collision from $v = 0 \rightarrow v = 1$ and from $v = 0 \rightarrow v = 6$. Compared to a rate of $2.5 \times 10^3 \text{ sec}^{-1} \text{ torr}^{-1}$ reported by Yardley⁷ for resonant VV transfer in CO at 120°K , the electron pumping rates are clearly much slower than those for vibrational cross-relaxation, and thus, it is the latter process that dominates the vibrational population distribution, and consequently the laser output spectrum.

Actually, the electron distribution function will not be Boltzmann. For the weakly ionized plasmas that are characteristic of electrical discharge laser systems, it is the inelastic vibrational and electronic excitation processes that dominate the kinetics of the electron gas. The structure of the electron distribution will typically reflect the structure of the electron-molecule energy exchange processes, and thus, it will depart most significantly from a Boltzmann in the energy regions where inelastic cross-sections are appreciable. For plasmas with mean electron energies of a few eV or less, elastic electron scattering and inelastic electron-molecule rotational excitation have a negligible effect on the determination of the distribution. Since the electrons in such low energy, weakly ionized plasmas have no mechanism for complete thermalization, a departure from a Boltzmann distribution is to be expected.

Nighan et al⁸⁻¹⁰ have carried out calculations for the electron distribution functions for various gas mixtures, based on the assumptions that the E/N of the plasma is low enough that the average electron energy is only a few eV and that all of the important inelastic electron-molecule excitation cross-sections are known. Knowledge of the electron energy distribution as a function of E/N and gas composition makes it possible to calculate the fractional amounts of the electrical energy input that is deposited into each of the electron-molecule excitation modes. For a fixed gas composition, the average electron energy will be a function only of E/N , and the fractional transfer of electrical input into vibrational or electronic energy states can be calculated as a function of this parameter. Clearly, it is desirable to operate at values of E/N which optimize the transfer of electrical energy to vibrational states, rather than to electronic states, and Nighan has shown that this is possible for many gas compositions typical of those used for CO_2 laser systems. These analyses show the extreme sensitivity of the vibrational excitation rates upon the plasma E/N and the gas constituents.

For the case of the CO₂ laser systems, the molecular kinetics are much simpler than for the case of CO, where many vibrational levels must be considered. The electron distribution function must depend upon the population of excited vibrational states of the molecular species if there exist inelastic excitation processes from such states that are important for extracting energy from the electron gas. Thus, a complete model for an electrical discharge CO laser would require a coupled set of equations for the molecular and electron kinetic processes, treated on an equal basis. Our experiments have shown that even the presence or absence of lasing may significantly change the electron distribution function; this was demonstrated by the fact that the visible CO emission from upper electronic states sharply increases when the laser cavity is blocked, suggesting that the average electron energy has been increased by the altered population distribution of the CO vibrational states. Since the vibrational population distribution is different when lasing is prohibited, the relative importance of the vibrational versus electronic state excitation mechanisms for the electron would be changed. Thus, for the CO laser it may not be possible to completely characterize the system only by the gas composition and the E/N of the plasma. For the case of CO₂ systems, extremely rapid cross-relaxation processes make it possible to describe the molecular kinetics in terms of only a very few molecular vibrational levels.

According to the measured cross-sections of Schulz⁶, electron excitation is effective only for ≤ 8 vibrational quanta. Using these cross-sections for CO Nighan has shown that the fractional electrical power transferred to CO vibrational levels is almost 100% for an average electron energy of $\sim .5$ eV and only about 15% for average electron energies ~ 3 eV. Qualitatively, the cross-sections for excitation of N₂ are quite similar to those for CO, although they are smaller by about a factor of six. Hence, N₂ would be expected to

have an effect on the electron distribution qualitatively similar (in energy dependence) to that for CO. Therefore, addition of N_2 to a CO laser mixture can be of benefit, since for the proper values of E/N , it would be as efficient for storing electrical energy in vibrational states as is CO. Since the levels of N_2 are nearly resonant with those for CO, this vibrational energy can be transferred by VV cross-relaxation to the CO levels and would not be lost (since VT relaxation is much slower). Two important factors to realize, however, are that N_2 can be added to alter the E/N of the plasma without loss of electron-vibration energy transfer efficiency, and its addition does not directly affect the CO-CO VV anharmonic pumping rates, which would have occurred if we had merely increased the CO partial pressure. Since VV pumping in the N_2 - N_2 system is probably much slower than that for N_2 -CO, most of the transfer from N_2 will be from the lowest level, viz. N_2 ($v = 1$).

The experimental results presented in the subsequent sections of this report support the mechanisms reviewed above.

4.0 MEASUREMENT OF CO LASER OPERATING CHARACTERISTICS

The experimental results presented here were obtained with a conventional longitudinal electric discharge configuration schematically shown in Figure 4.1. The quartz discharge tube had an i. d. of 2.1 cm with an electrode separation of 124 cm. The resonator was formed by two mirrors, a 10 m total reflector, and a partially transmitting plane mirror. The multimode resonator volume was approximately the total discharge volume. The discharge tube could be cooled with water or liquid nitrogen passed through an outer jacket.

The two ends of the discharge tube were fitted to Brewster window holders with O-rings. Alternatively, the ends could be fitted to metal mirror mounts with bellows, also provided with O-rings. Salt, barium fluoride, or Irtran Brewster windows were also mounted with O-ring seals. This arrangement with O-ring seals, schematically shown in Figure 4.2, was found to be very convenient for insuring stability of the laser in spite of changes in tube length with temperature. For further stability, the laser tube and the optical components were mounted on a granite rail.

The laser was excited by a μ c power supply provided with an electronic current controller. Since the discharge current in a CO laser is found to fluctuate quite frequently, the electronic current controller was found to be essential for obtaining a stable output. The laser output power was measured by a Coherent Radiation Laboratory power meter calibrated against an Epply thermopile.

The gases were mixed in a mixing manifold fitted with flowmeters for individual gases. The gas mixtures were pumped with a partially throttled Welch Duoseal Vacuum Pump Model 1397B with a pumping capacity of 500 liters/min. The pressure of the tube was monitored at the inlet and

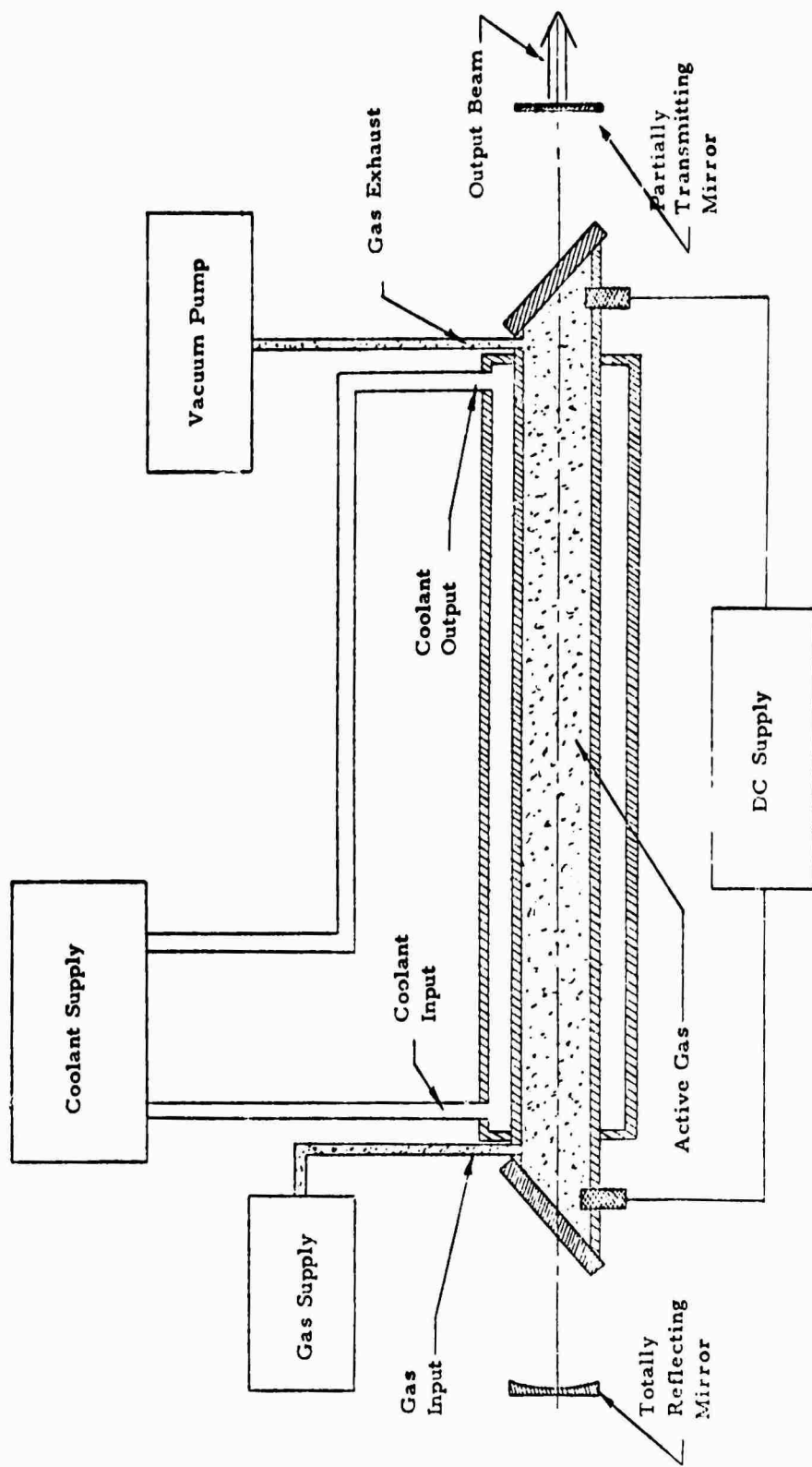


Figure 4.1 Schematic of the CO Laser

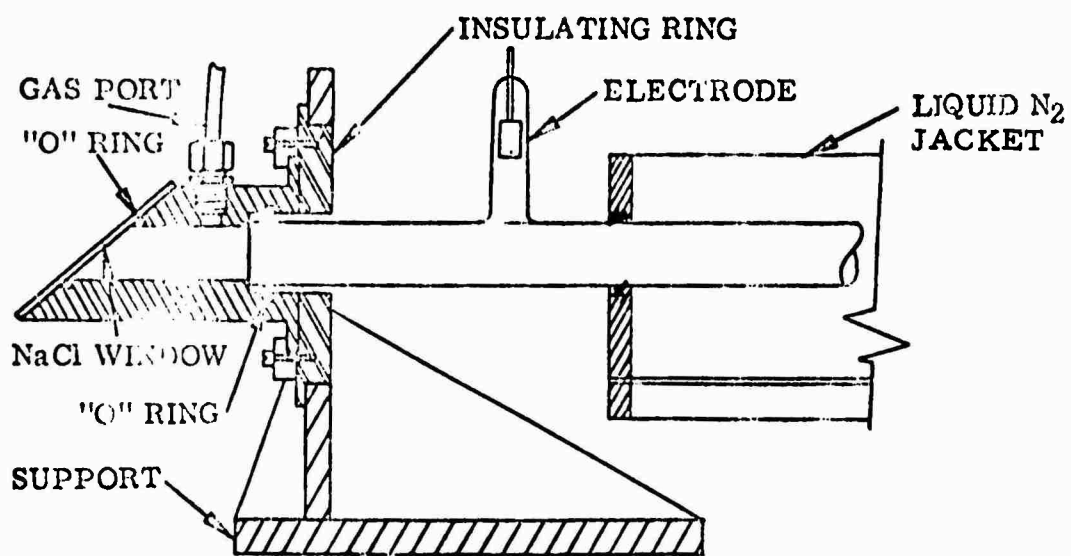


Figure 4.2 Typical End Detail of the Discharge Tube

exhaust ends of the discharge tube with Wallace and Tiernan gauges. Whenever a higher accuracy was needed, the partial pressures of the gas mixture were measured by a Pace variable reluctance differential pressure transducer with an accuracy of $\pm 5\%$.

The gas composition and the power outputs at four different wall temperatures are shown in Table I. The optimum gas mixture necessary for highest efficiency was found to be different for different temperatures. The efficiency at room temperature was found to be 12.1%. With addition of Hg to the gas mixture, the efficiency increased to 18%. The data in Table I also demonstrates the beneficial effect of adding Xe. As discussed in Sections 3 and 5, the enhancement in efficiency with addition of Xe and Hg is believed to be due to the lower electron temperature with Xe and Hg which better matches the energy of the peak cross-sections for vibrational excitation due to electron impact.

The maximum efficiency obtained by optimizing the gas mixture at each temperature is plotted in Figure 4.3 as a function of temperature. The cavity configuration was the same as that of C in Table I. The efficiency is found to increase with decreasing temperature.

The highest efficiency of 46.9%, corresponding to a CW output power of 70W, was obtained at 77°K wall temperature using internal mirrors. From Nighan's calculations¹⁰ it is estimated that for the value of E/N at which the laser was operated, 60% of the electrical input energy was transferred to the vibrational states of the CO and N₂ molecules. Therefore, total efficiency of 47% implies nearly 80% conversion efficiency from vibrational energy to coherent radiation.

TABLE I. CO LASER OPERATING CHARACTERISTICS

Configuration and Wall Temperature	Pressure (Torr)					Xe	Discharge Voltage kV	Discharge Current mA	Output Watts	Efficiency Percent
	Total	He	CO	N ₂	O ₂					
D77°K	18	16	0.5	1.5	0.01	0.3	12.4	12	70	46.9
A77°K	16.00	15	0.4	0.4	0.01	.15	12.8	10	51	39.8
A77°K	16.1	15.25	0.25	0.6	0.01	-	13.6	18	60	29.2
A77°K	16.25	15.25	0.25	0.6	0.01	.15	12.8	18	70	36.7
B77°K	17.3	14.9	1.6	1.8	0.01	-	12.0	27	91	28
B150°K	18.32	14.9	1.5	1.9	0.02	-	12.0	10	25	20.8
C220°K	16.26	12.5	0.45	3.0	0.02	0.3	9.0	22.5	42.5	21
C300°K	15.97	12.5	0.45	3.0	0.02	-	14	13	10	5.5
C300°K	16.26	12.5	0.45	3.0	0.02	0.3	9.2	22.5	25	12.1
E300°K	16.36	12.5	0.45	3.0	0.02	0.4	14	12	12.5	7.0

Configuration:

Discharge length 126 cm; cooling jacket 115 cm; a 10 meter total reflector and a plane output mirror of reflectivity R in each case; cavity length for A, B and C is 215 cm with two Brewster windows; cavity length for D and E is 165 cm with internal mirrors.

Values of R: A = 95%, B = 90%, C = 85%, D = 80%, E = 85%.

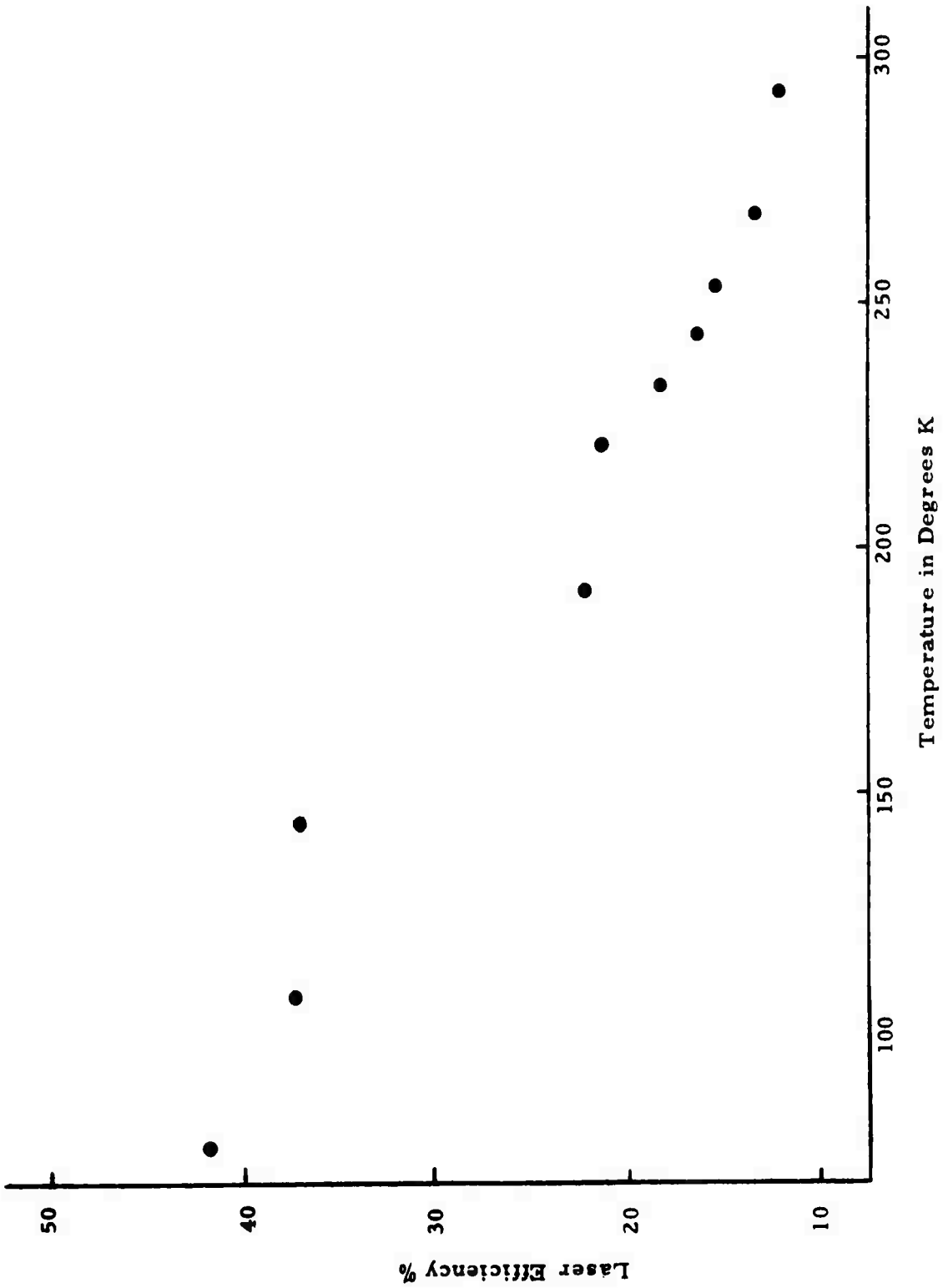


Figure 4.3 Maximum laser efficiency vs. wall temperature obtained by optimizing both the gas mixture (including Xe) and the current, using cavity configuration C of Table I

5.0 THE ROLE OF VARIOUS GAS CONSTITUENTS

The operating characteristics of the CO laser presented in the last section show that the optimum gas mixture contains several other constituents in addition to CO. In a slowly flowing system, He is well known to be beneficial for cooling the molecular kinetic temperature. The effect of Xe is to reduce the average electron energy by lowering the high energy tail of the electron energy distribution. Use of Xe is, therefore, a crude method for altering the E/N of the discharge. Since Xe has the lowest ionization potential of any of the constituents typically used in a CO laser mixture, it may also be useful for preventing CO decomposition due to collisions with high energy electrons.

As discussed in Section 3, N₂ may also serve the function of lowering the average electron energy (or, equivalently, the plasma E/N). The beneficial effects that result from the simultaneous presence of N₂ and Xe may be due to the fact that N₂ and Xe alter the plasma characteristics in qualitatively different ways. For example, the fractional conversion of electrical to vibrational energy is improved not only upon lowering the E/N, but is evidently enhanced also by an optimum gas composition, since the performance can be improved by the simultaneous presence of both of these constituents. An equivalent enhancement cannot be obtained merely by increasing the fractional amount of Xe in the gas mixture. It may be possible that the effect of N₂ can be understood on the basis of the discussion given in Section 3 i. e., it may serve as a way of altering the E/N without changing the qualitative structure of the electron energy distribution from that of pure CO. Since the addition of N₂ does not cause degradation of the fractional transfer of energy to vibrations, it may have advantages that an addition of Xe cannot provide. For the plasma characteristics, the effect of the addition of N₂ could probably be accomplished equivalently by increasing the partial

pressure of CO (although the average electron energy would not be the same function of E/N). However, the optimum concentration of CO in the laser mixture is also determined by other constraints, such as the rate of VV pumping, VT relaxation, decomposition, etc. Thus, the optimum mixture seems to require several ingredients (typically CO, N₂, He and Xe).

The addition of O₂ often plays a very sensitive role, inasmuch as very small amounts can have a critical effect on the operation. A small amount of O₂ is helpful, because it probably minimizes CO decomposition by driving the reaction $\text{CO} \rightleftharpoons \text{C} + \text{O}$ to the left and prohibits carbon deposits. Beyond a critical amount, the presence of O₂ can have a deleterious effect on the laser performance. This may be due to a drastic alteration of the plasma characteristics (since O₂ has a large electron attachment coefficient of magnitude greater than that for most gases), or it may result in the formation of CO₂ (at least for room temperature operation). Since such minute amounts can have such an important effect, the former explanation is probably correct.

Osgood et al¹¹ have suggested that the beneficial effect of adding O₂ to the electrically excited CO laser is due to removal of CN radicals by oxidation. The CN radical is believed to be deleterious in CO lasers since the vibrational energy of the CO molecules may be transferred to the excited electronic states of CN where it is quickly dissipated as visible fluorescence. The following arguments are presented against this hypothesis:

1. A small amount of O₂ (or NO) is seen to be equally beneficial even when there is no nitrogen present in the gas mixture to produce CN.
2. The amount of CN formation in an electric discharge is quite small. The amount of visible CN emission intensity observed in the side-light may be misleading, since even a small amount of CN could give a strong fluorescence.

3. The energy transfer from vibrationally excited CO to electronic states of CN involves simultaneous change in 12 vibrational quantum numbers in CO. Such a transfer can be efficient only in short range encounters which would be rather few due to the low concentration of CN expected in the discharge.

4. Addition of O₂ not only reduces the CN emission, it also strongly reduces the visible sidelight emission in general.

Because of the above arguments, it may be concluded that while the addition of O₂ may decrease the formation of CN, the primary beneficial effect of adding oxygen must be due to some other effect such as preventing the CO decomposition, described earlier.

One final note of caution is that CO laser performance is extremely sensitive to the cleanliness of the system; leaks of impurities such as O₂, H₂O vapor or H₂ can completely quench the oscillation, especially at room temperatures. In the early development of the CO laser, addition of too much O₂ in LN₂-cooled systems was responsible for formation of ozone freeze-out, and several workers experienced dangerous explosions caused by rapid expansion of the ozone as it warmed up. This problem is completely eliminated by adding judicious amount of O₂.

6.0 SPECTRAL MEASUREMENTS

The energy level and spectroscopy of the CO molecule have been discussed in detail in the accompanying theoretical report¹. Briefly, the infrared spectrum of the CO molecule arises from transitions between vibrational rotational levels obeying proper selection rules. The selection rules for electric dipole radiation emission lead to allowed transitions for $v \rightarrow v-1$ and $J \pm 1 \rightarrow J$ where v and J are the vibrational and rotational quantum numbers. The transitions are denoted as $v \rightarrow v-1$, P(J) for $J-1 \rightarrow J$ and R(J) for $J+1 \rightarrow J$, respectively.

6.1 Measurement of Laser Output Spectra at Various Temperatures

For these measurements, a laser tube similar in all respects to that described in Section 4.0 (but without a cooling jacket) is utilized. Instead, the tube was immersed in a temperature control bath for which the wall temperature could be maintained at any selected temperature between 77°K and ambient by controlling the flow of cold N₂ gas through a bath containing a mixture of equal parts of 2-methylbutane and isohexane. The laser gas mixture consisted of CO-N₂-He-O₂ with partial pressures of 0.35, 2.1, 12.0, 0.01 torr. The laser output spectra were recorded by a SPEX 1600 spectrometer equipped with a 150 line/mm grating blazed at 6 μ .

A computer program has been written to calculate the P and R transition frequencies for $v = 1$ to 30 and $J = 1$ to 50. The band and branch label of the transitions responsible for an observed frequency could then be identified, since the output was numerically sorted.

The spectrometer was calibrated using different orders of a He-Ne as well as an Argon ion laser. The spectra were taken every 10°K between 300°K and 77°K; the observed transitions at different temperatures are listed in Table II. No attempt was made to optimize the power at each temperature.

TABLE II. CO LASER SPECTRA AT VARIOUS TEMPERATURES

Temperature: 20°C

Output: 8 watts

Vibrational Band	Transition	$\lambda(\mu)$ (Air)	Relative Intensity	cm^{-1}
8-7	P(20)	5.3152	80	1880.897
	P(21)	5.3273	9	1876.629
	P(22)	5.3395	10	1872.329
9-8	P(20)	5.3876	100	1855.615
	P(21)	5.3999	16	1851.382
10-9	P(17)			1842.821
	P(19)	5.4494	52	1834.577
11-10	P(18)	5.5127	17	1813.514
	P(19)	5.5252	1.8	1809.416
12-11	P(18)	5.5901	2.2	1788.398
	P(19)	5.6028	0.9	1784.334
13-12	P(17)	5.6567	0.3	1767.359
	P(18)	5.6695	0.5	1763.363
	P(19)	5.6825	---	1759.334
14-13	P(14)	5.6996	0.3	1754.060

Temperature: 0°C

Output: 6 watts

9-8	P(18)	5.36342	.16	1863.985
	P(19)	5.37545	.71	1859.816
	P(20)	5.38762	.19	1855.615
10-9	P(17)	5.42505	1.00	1842.812
	P(19)	5.44940	.76	1834.577
11-10	P(18)	5.51269	.98	1813.514
	P(19)	5.52518	.57	1809.416
12-11	P(18)	5.59011	.71	1788.398
	P(19)	5.60284	.25	1784.334
13-12	P(17)	5.65666	.50	1767.359
	P(18)	5.66948	.23	1763.363

CO LASER SPECTRA AT VARIOUS TEMPERATURES

Temperature: -40°C

Output: 8 watts

Vibrational Band	Transition	$\lambda(\mu)$ (Air)	Relative Intensity	cm^{-1}
8-7	P(19)	5.30326	.88	1885.133
	P(20)	5.31520	.77	1880.897
9-8	P(18)	5.36342	.79	1863.985
	P(19)	5.37545	.80	1859.816
	P(20)	5.38762	.23	1855.615
10-9	P(17)	5.42505	1.00	1842.812
	P(19)	5.44940	.68	1834.577
11-10	P(16)	5.48818	.15	1821.615
	P(17)	5.50036	.11	1817.581
	P(18)	5.51269	.78	1813.514
	P(19)	5.52518	.31	1809.416
12-11	P(18)	5.59011	.72	1788.398
	P(19)	5.60284	.19	1784.334
13-12	P(17)	5.65666	.46	1767.359
	P(18)	5.66948	.11	1763.363
14-13	P(17)	5.73778	.28	1742.371

Temperature: -60°C

Output: 11 watts

7-6	P(19)	5.23277	.26	1910.525
	P(20)	5.24450	.67	1906.254
8-7	P(19)	5.30326	1.00	1885.133
	P(20)	5.31520	.53	1880.897
9-8	P(18)	5.35342	1.00	1863.985
	P(19)	5.37545	.62	1859.816
10-9	P(17)	5.42505	1.00	1842.812
	P(19)	5.44940	.33	1834.577

CO LASER SPECTRA AT VARIOUS TEMPERATURES

Temperature: -60°C (Cont.)Output: 11 watts

Vibrational Band	Transition	$\lambda(\mu)$ (Air)	Relative Intensity	cm^{-1}
11-10	P(16)	5.48818	.77	1821.615
	P(17)	5.50036	.11	1817.581
	P(18)	5.51269	.58	1813.514
	P(19)	5.52518	.14	1809.416
12-11	P(15)	5.55286	.24	1800.394
	P(18)	5.59011	.66	1788.398
	P(19)	5.60284	.08	1784.334
13-12	P(17)	5.65666	.51	1763.363
14-13	P(15)	5.71213	.08	1750.196
	P(17)	5.73778	.24	1742.371

Temperature: -80°COutput: 13.5 watts

7-6	P(18)	5.22119	.87	1914.764
	P(19)	5.23277	.51	1910.525
	P(20)	5.24450	.39	1906.254
8-7	P(17)	5.27980	1.00	1893.509
	P(19)	5.30326	1.00	1885.133
9-8	P(16)	5.33982	.43	1872.226
	P(18)	5.35342	1.00	1863.985
	P(19)	5.37545	.18	1859.816
10-9	P(17)	5.42505	1.00	1842.812
11-10	P(16)	5.48818	1.00	1821.615
	P(17)	5.50036	.14	1817.581
	P(18)	5.51269	.07	1813.514
12-11	P(15)	5.55286	.72	1800.394
	P(18)	5.59011	.14	1788.398
13-12	P(15)	5.63150	.21	1775.254
	P(17)	5.65666	.20	1763.363
14-13	P(14)	5.69955	.28	1754.060
	P(15)	5.71213	.09	1750.196

CO LASER SPECTRA AT VARIOUS TEMPERATURES

Temperature: -100°C

Output: 17 watts

Vibrational Band	Transition	$\lambda(\mu)$ (Air)	Relative Intensity	cm^{-1}
7-6	P(17)	5.20974	.15	1918.971
	P(18)	5.22119	.72	1914.764
8-7	P(17)	5.27980	.89	1893.509
	P(19)	5.30326	.61	1885.133
9-8	P(16)	5.33982	.37	1872.226
	P(18)	5.36342	1.00	1863.985
10-9	P(15)	5.40129	.18	1850.917
	P(16)	5.41309	.12	1846.881
	P(17)	5.42505	.88	1842.812
11-10	P(16)	5.48818	.99	1821.615
	P(17)	5.50036	.11	1817.581
12-11	P(15)	5.55286	.33	1800.394
13-12	P(15)	5.63150	.10	1775.254
	P(17)	5.65666	.08	1763.363
14-13	P(14)	5.69955	.11	1754.060
	P(15)	5.71213	.08	1750.196

Temperature: -120°C

Output: 20 watts

7-6	P(17)	5.20974	.22	1918.971
	P(18)	5.22119	1.00	1914.764
	P(19)	5.23277	.13	1910.525
8-7	P(17)	5.27980	1.00	1893.509
9-8	P(16)	5.33982	1.00	1872.226
	P(18)	5.36342	.24	1863.985
10-9	P(15)	5.40129	.58	1850.917
	P(16)	5.41309	.11	1846.881
	P(17)	5.42505	.76	1842.812

CO LASER SPECTRA AT VARIOUS TEMPERATURES

Temperature: -120°C (Cont.)

Output: 20 watts

Vibrational Band	Transition	$\lambda(\mu)$ (Air)	Relative Intensity	cm^{-1}
11-10	P(16)	5.48818	.83	1821.615
12-11	P(14)	5.54076	.28	1804.328
	P(15)	5.55286	.30	1800.394
13-12	P(13)	5.60698	.22	1783.018
	P(15)	5.63150	.18	1775.254
14-13	P(13)	5.68712	.16	1757.890
	P(14)	5.69955	.12	1754.060

Temperature: -140°C

Output: 22 watts

6-5	P(18)	5.15256	.24	1940.266
	P(19)	5.16394	.08	1935.992
7-6	P(17)	5.20974	.91	1918.971
	P(18)	5.22119	.45	1914.764
8-7	P(16)	5.26828	.40	1897.648
	P(17)	5.27980	1.00	1893.509
9-8	P(15)	5.32823	.45	1876.297
	P(16)	5.33982	.88	1872.226
	P(18)	5.36342	.11	1863.985
10-9	P(14)	5.38963	.08	1854.921
	P(15)	5.40129	.25	1850.917
	P(16)	5.41309	.49	1846.881
	P(17)	5.42505	.22	1842.812
11-10	P(15)	5.47615	.19	1825.616
	P(16)	5.48818	.32	1821.615
12-11	P(14)	5.54076	.41	1804.328
	P(15)	5.55286	.42	1800.394
13-12	P(13)	5.60698	.23	1783.018
	P(15)	5.63150	.15	1775.254
14-13	P(14)	5.69955	.22	1754.060

CO LASER SPECTRA AT VARIOUS TEMPERATURES

Temperature: -160°COutput: 23 watts

Vibrational Band	Transition	$\lambda(\mu)$ (Air)	Relative Intensity	cm^{-1}
6-5	P(17)	5.14132	.51	1944.508
	P(18)	5.15256	.32	1940.266
7-6	P(15)	5.18726	.69	1927.287
	P(17)	5.20974	1.00	1918.971
	P(18)	5.22119	.50	1914.764
8-7	P(14)	5.24567	.27	1905.829
	P(15)	5.25690	.40	1901.755
	P(16)	5.26828	.62	1897.648
	P(17)	5.27980	.88	1893.509
9-8	P(14)	5.31678	.65	1880.336
	P(15)	5.32823	.95	1876.297
	P(16)	5.33982	.62	1872.226
10-9	P(14)	5.38963	.64	1854.921
	P(15)	5.40129	.35	1850.917
	P(16)	5.41309	.34	1846.881
11-10	P(13)	5.45254	.34	1833.521
	P(15)	5.47615	.26	1825.616
	P(16)	5.48818	.22	1821.615
12-11	P(13)	5.52880	.22	1808.229
	P(14)	5.54076	.54	1804.328
13-12	P(13)	5.60698	.36	1783.018
14-13	P(13)	5.68712	.22	1757.890
	P(14)	5.69955	.23	1754.060

Temperature: -183°COutput: 22 watts

6-5	P(14)	5.10840	.43	1957.039
	P(16)	5.13022	.26	1948.717
	P(17)	5.14132	.43	1944.508

CO LASER SPECTRA AT VARIOUS TEMPERATURES

Temperature: -183°C (Cont.)Output: 22 watts

Vibrational Band	Transition	$\lambda(\mu)$ (Air)	Relative Intensity	cm^{-1}
7-6	P(15)	5.18726	1.00	1927.287
	P(17)	5.20974	.37	1918.971
	P(18)	5.22119	.25	1914.764
8-7	P(14)	5.24567	.40	1905.829
	P(15)	5.25690	.46	1901.755
	P(16)	5.26828	.47	1897.648
	P(17)	5.27980	.44	1893.509
9-8	P(13)	5.30548	.22	1884.342
	P(14)	5.31678	.32	1880.336
	P(15)	5.32823	.66	1876.297
	P(16)	5.33982	.37	1872.226
10-9	P(13)	5.37812	.23	1858.892
	P(14)	5.38963	.39	1854.921
	P(15)	5.40129	.46	1850.917
	P(16)	5.41309	.22	1847.881
11-10	P(13)	5.45254	.42	1833.521
12-11	P(13)	5.52880	.20	1808.229
	P(14)	5.54076	.35	1804.328

6.2 Observation of Anharmonic Pumping. The output spectra at four different temperatures for which significant changes were observed have been selected from the spectral data presented in the previous section, and are presented in Figure 6.1.

It is observed that the CO laser spectrum shifts toward lower vibrational transitions as the molecular kinetic temperature is reduced. Qualitative evidence of anharmonic pumping can be inferred from this observation, by means of the following simple argument. Since CO has a small anharmonic defect, the energy spacing between the vibrational levels becomes successively smaller. Since most of the excited CO molecules are in the lowest states, the distribution of input energy into the higher vibrational states proceeds mainly by collisions with CO ($v = 1$), such as $\text{CO}(v-1) + \text{CO}(1) \rightarrow \text{CO}(v) + \text{CO}(0) + \Delta E$. The excess energy, $\Delta E = 2\omega_e x_e (v-1)$ is transferred to kinetic energy, and by detailed balance, the rate for the reverse process is reduced by a factor $\exp(-\Delta E/kT_{\text{mol}})$. (The reverse process requires energy to be supplied by the translational mode, so its rate will be slower, because there are fewer molecules with higher kinetic energies.) When the energy discrepancy ΔE becomes comparable to or greater than kT_{mol} , there will be a "trapping" effect whereby molecules are inhibited from relaxing by collisions with CO ($v = 0$). Such an effect is evident from the data presented in Table III which shows the correlation between the threshold band and the gas temperature.

The gas temperatures were calculated by the expression

$$Q(T_g) = 18.9 (T_g - T_w) \lambda_T (T_g)$$

where $Q(T)$ is the heat input to the gas per unit time per unit length of the

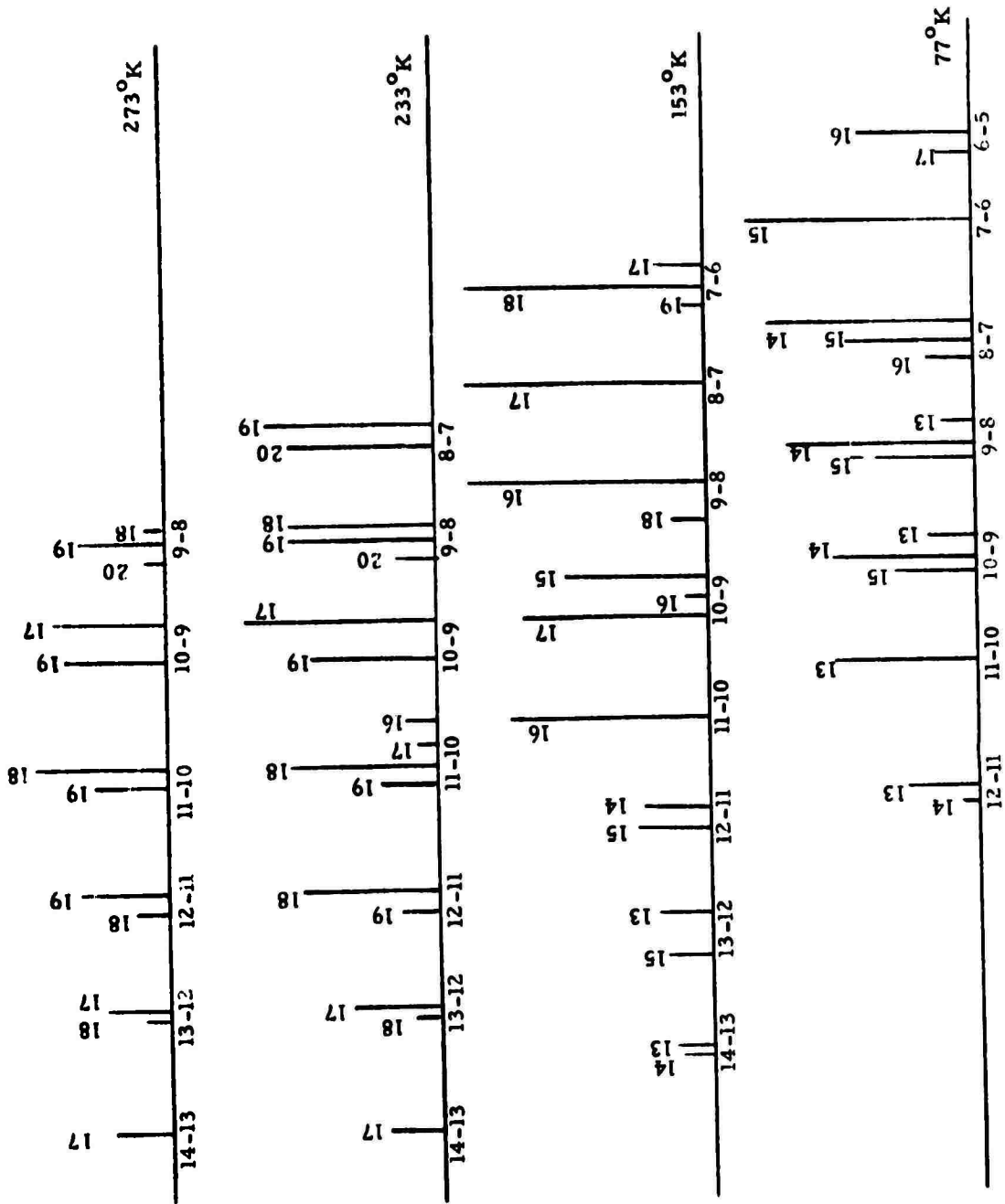


Figure 6.1 CO Laser Spectra at Various Wall Temperatures

TABLE III. CORRELATION BETWEEN THE GAS TEMPERATURE
AND THE THRESHOLD BAND

Input Power	Output Power	Heat Input	T_w	T_g	v_g	Observed
Watts	Watts	Watts	$^{\circ}K$	$^{\circ}K$		Threshold Band
160	20	140	77	197	6	6 - 5
160	25	135	153	228	7	7 - 6
120	6	114	233	280	8	8 - 7
130	2	128	273	322	9	9 - 8

laser tube; T_g and T_w are the gas and the wall temperatures, respectively; λ_T is the thermal conductivity of the gas, assumed to be pure He in this case, since 80% of the mixture was He. The heat input per second was taken to be simply the difference between the input and the output powers. The vibrational level v_g for which $\Delta E = 2\omega_e x_e (v_g - 1) \approx kT_g$, is calculated from the gas temperature T_g . Finally, the experimentally observed lowest vibrational band at the gas temperatures are listed in Table III.

At a gas temperature of 200°K, the lowest vibrational band to appear is 6-5, and this gradually shifts to higher and higher vibrational bands as the temperature is increased. Throughout the entire temperature range, the appearance of the threshold band for lasing at a given kinetic temperature is in excellent agreement with the expectation from the "trapping" effect discussed above, and thereby clearly indicates the manifestation of anharmonic pumping.

6.3 Time Resolved Spectroscopic Measurements. It should be noticed from Figure 6.1 that the output spectra consist, in many cases, of more than one rotational transition for a given vibrational band. This results from the rate of stimulated emission due to cascading being comparable to, or greater than, that of rotational cross-relaxation. Such a conclusion is clearly demonstrated by a study of time-resolved spectroscopy of a Q-switched CO laser, where this effect was also observed. For this study, a dc discharge was maintained, with a chopper to block the laser cavity. By scanning the spectrometer wavelength with the chopper running, the delay times for the appearance of various vibrational-rotational transitions were measured using the display on an oscilloscope (triggered synchronously by the chopper). In this way, it was possible to obtain a measurement of the delay time, for any given transition.

It was observed that, after a delay time of $2.6 \mu\text{sec}$, a cascade of lines (Figure 6.2) appeared simultaneously, corresponding to the chain of transitions from $5 \rightarrow 4$ P(15) to $9 \rightarrow 8$ P(11). The lines corresponding to a second chain from $5 \rightarrow 4$ P(16) to $7 \rightarrow 6$ P(14) appeared at a later time delayed by $3.6 \mu\text{sec}$. Another chain beginning at $5 \rightarrow 4$ P(17) and ending in $8 \rightarrow 7$ P(14) appeared at a delay time of $4 \mu\text{sec}$ after opening the shutter. The first cascade appearing at a delay time of $2.6 \mu\text{sec}$ also reappeared whenever another cascade was proceeding, viz., at 3.6 and $4 \mu\text{sec}$, although with lower intensity. This shows that some energy leaks into neighboring rotational levels during cascading because of the sudden increase in population in certain rotational levels taking part in the cascade. The time sequence in which the various cascades start seems to be the result of different gain in those lines. The interesting fact to note is that during the interval of $1 \mu\text{sec}$ between the first and the second cascade, the stimulated emission competes with rotational cross-relaxation and the rate for the former is higher. With partial pressure of 15 torr there are about 170 collisions in $1 \mu\text{sec}$. Thus, the results indicate that the rotational thermalization of CO (with mostly He) requires more than 170 collisions in presence of competing stimulated emission.

The rate of rotational cross-relaxation in CO is therefore quite low compared to that in CO_2 , where only a few collisions are needed for rotational thermalization. This result is not surprising considering the fact that the rotational level spacing in CO is about 5 times larger and the molecular kinetic energy is lower at 77°K .

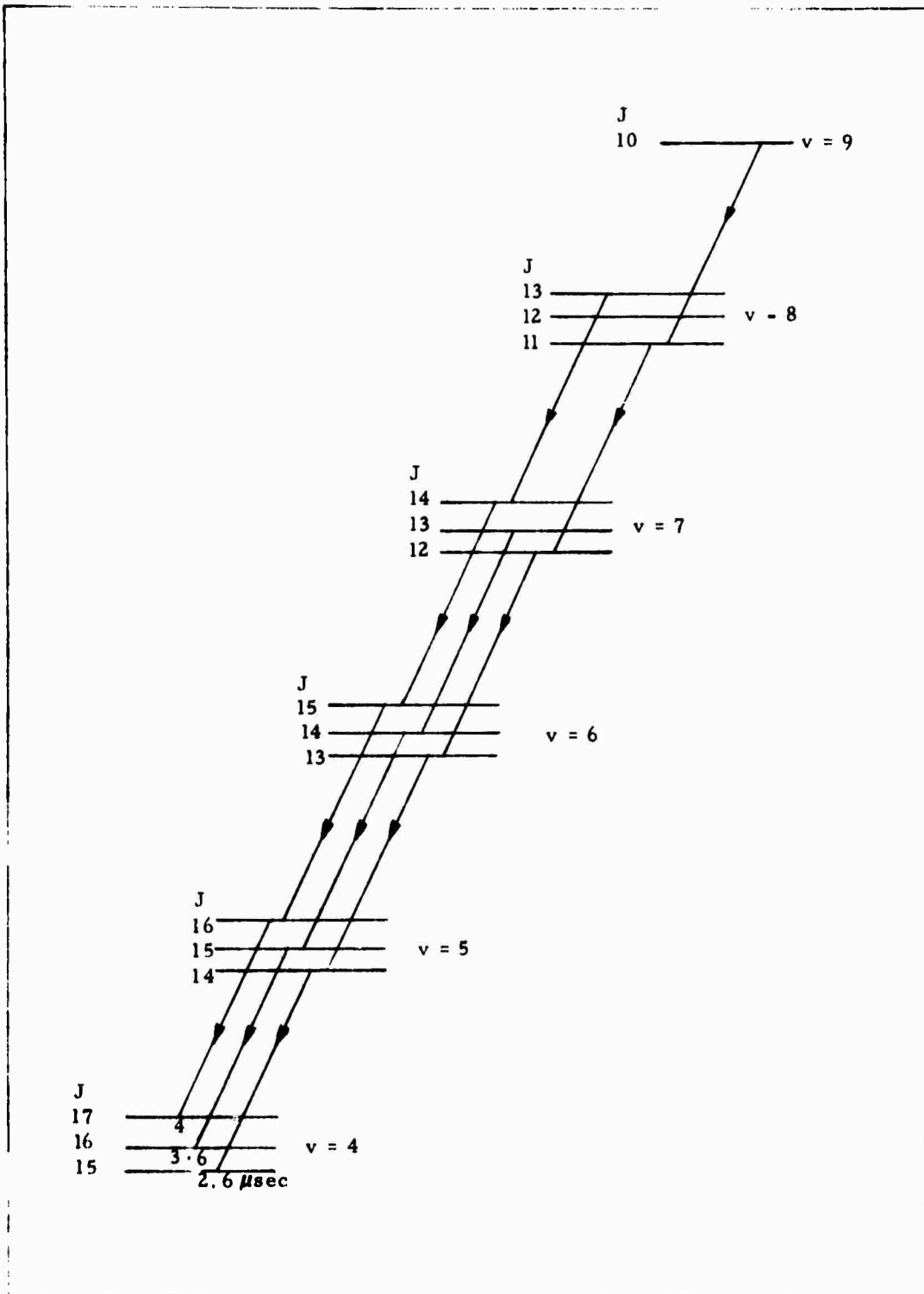


Figure 6.2 Cascading Phenomena in CO Laser; three cascades are shown appearing at a delay time of 2.6, 3.6, and $4 \mu\text{sec}$

7.0 GAIN MEASUREMENT AND ANALYSIS

Measurement of small signal gain makes it possible to determine the populations associated with different vibrational levels. Therefore, gain measurements provide the most direct method for testing the theoretical model of pumping and relaxation mechanisms. For this reason, a considerable effort was spent in obtaining precisely measured gain data.

The small signal gain coefficient α_o is given by

$$\alpha_o = \frac{1}{I} \frac{dI}{dz}$$

where I is the input intensity, and dI is the change in the intensity in a length dz . Since the measured gains are low, α_o can be simply given by

$$\alpha_o = \frac{I_2 - I_1}{I_1 L}$$

where $I_2 - I_1$ is the change in intensity in a gain length L .

7.1 Small Signal Gain Measurement. Using the experimental apparatus shown in Figure 7.1, small signal gains for LN_2 and room temperature operation of a CO amplifier were measured. The various vibrational-rotational lines were selected by terminating the oscillator cavity with a grating. The output mirror was mounted on a PZT mount to stabilize the oscillator cavity and to keep the output laser frequency on the line center. The PZT mount was controlled by a feedback loop with a Lansing stabilizer. The lasing lines were identified with a Spex 1800 spectrometer, and the amplified beam was detected with an Epply thermopile, Ge: Au or InSb detector. Signal processing was accomplished with a PAR 160 boxcar integrator. The amplified intensity was measured with the discharge in the gain tube turned on while the initial intensity was measured with the

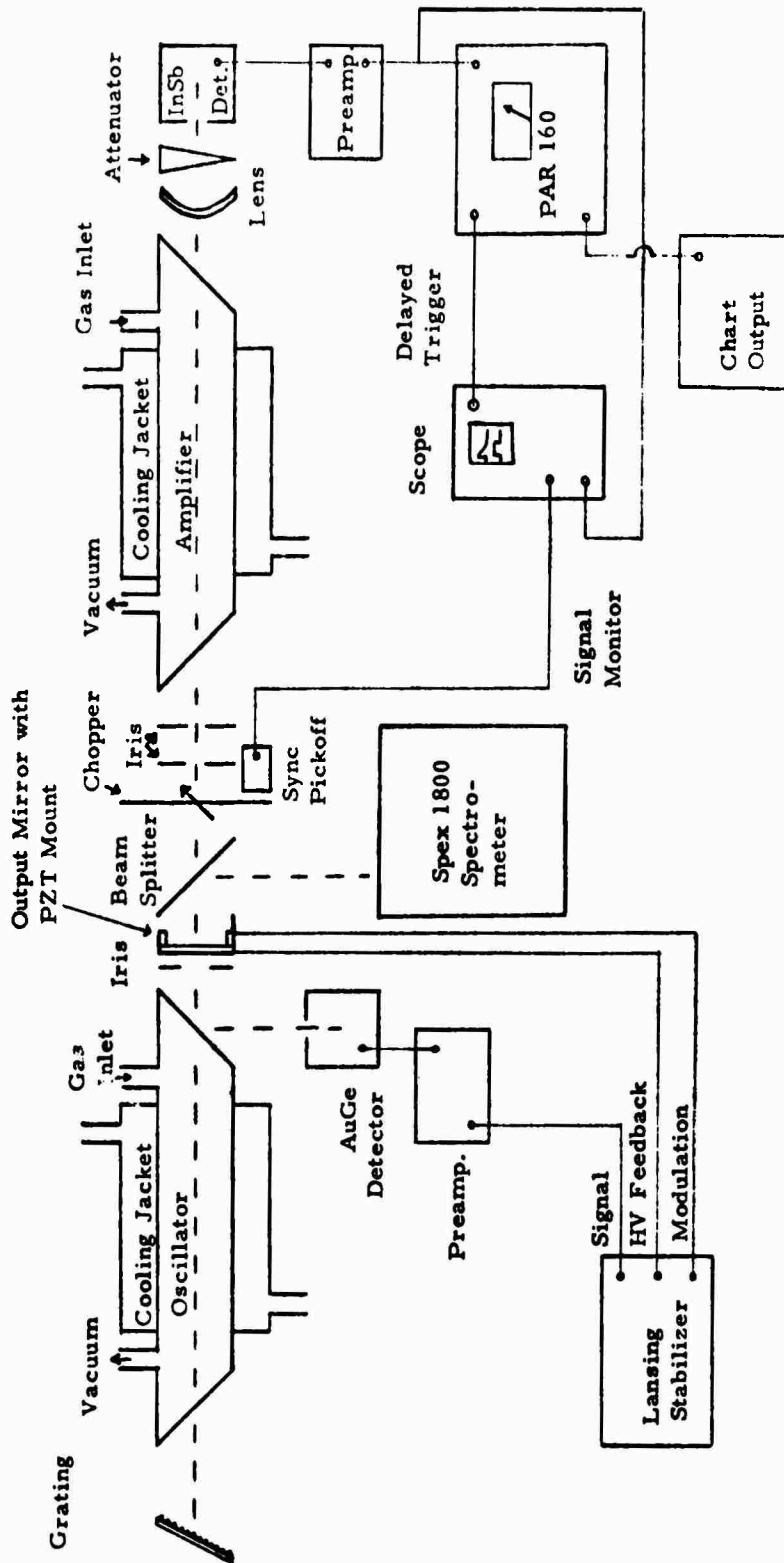


Figure 7.1 Experimental Configuration for CO Laser Gain Measurement

gain tube switched off. The amplified intensity was corrected for the spontaneous fluorescence coming from the amplifier tube. The gas mixture for operation at 77°K was 0.18 torr CO, 0.26 torr N₂, 12 torr He and 0.01 torr O₂ while that for 300°K was 1.1 torr CO, 6.5 torr N₂, 15 torr He and 0.02 torr O₂.

Figure 7.2 shows the results of the gain measurement at a 77°K wall temperature. The gain in any particular vibrational band varies as a function of the rotational level of the transition. The peak small signal gain is seen to vary from .005 cm⁻¹ for the 6→5 band, to 0.017 cm⁻¹ for the 12→11 band. In multiline operation (v = 10→9 to v = 6→5), the gain was found to be typically 0.0064 cm⁻¹. Figure 7.3 shows the results of gain measurements at room temperature; the gain is lower by an order of magnitude from the values at 77°K. However, with the addition of xenon, the room temperature gains were found to increase by about 50% for each of the values shown in Figure 7.3.

7.2 Interpretation of Gain Measurements. The small signal gain coefficient α for a Doppler broadened P(J) transition from v → v - 1 is given by the expression:

$$\alpha_{v \rightarrow v-1} P(J) = \frac{8\pi^3 c}{3kT} \left(\frac{M}{2\pi RT} \right)^{1/2} J v |R_{10}|^2 \left\{ N_v B_v e^{-B_v J(J-1)hc/kT} - N_{v-1} B_{v-1} e^{-B_{v-1} J(J+1)hc/(kT)} \right\},$$

where k is the Boltzmann constant, T the molecular temperature, c the velocity of light, M the gram molecular mass; R the gas constant, N_v and N_{v-1} the population densities of the upper and the lower levels, and where |R₁₀|², the square of the matrix element for the vibrational transition v = 1 → v = 0, is taken to be 9.8 x 10⁻³⁹ esu. The Doppler linewidth has been

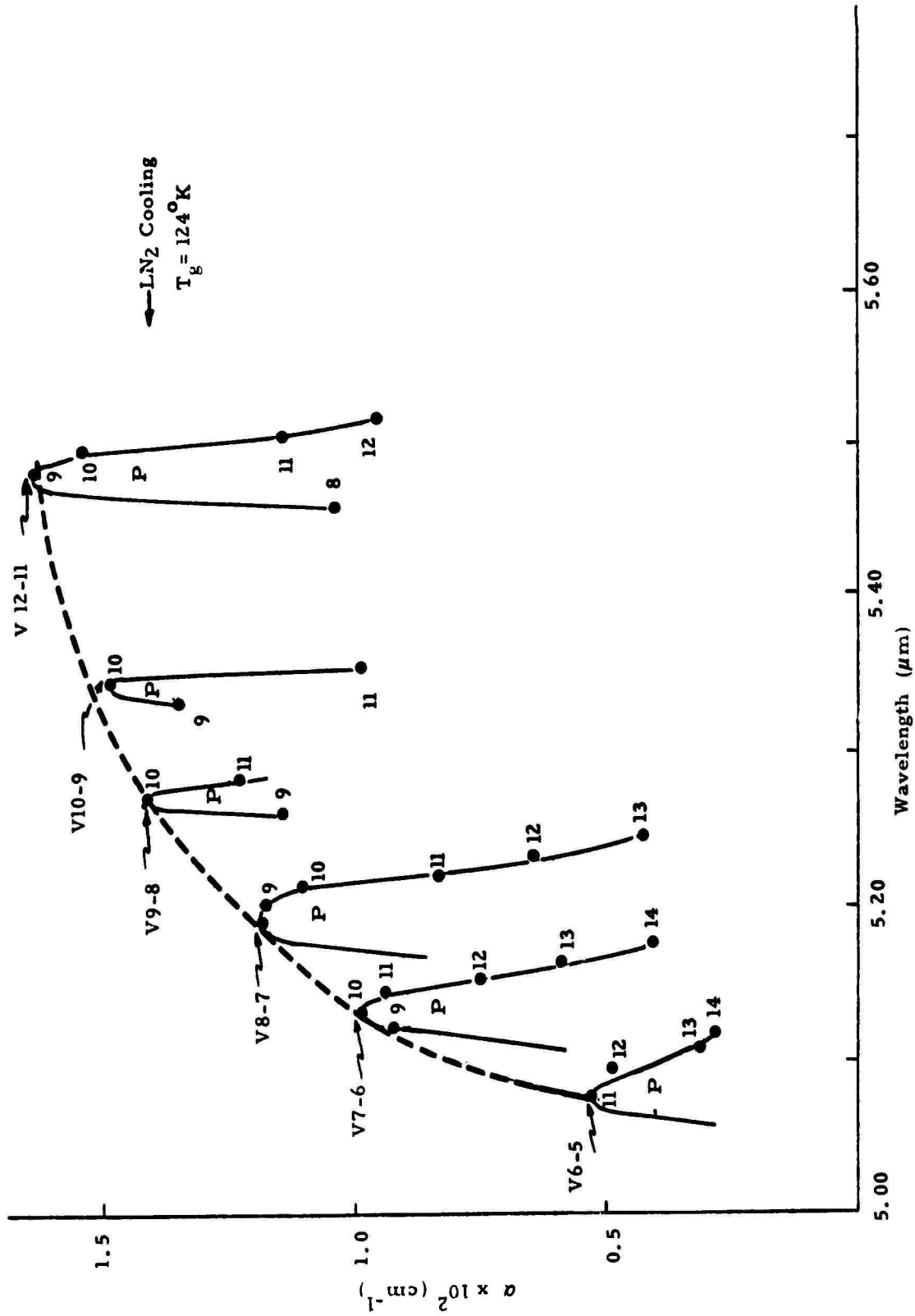


Figure 7.2 CO Laser Gains at 77°K Wall Temperature

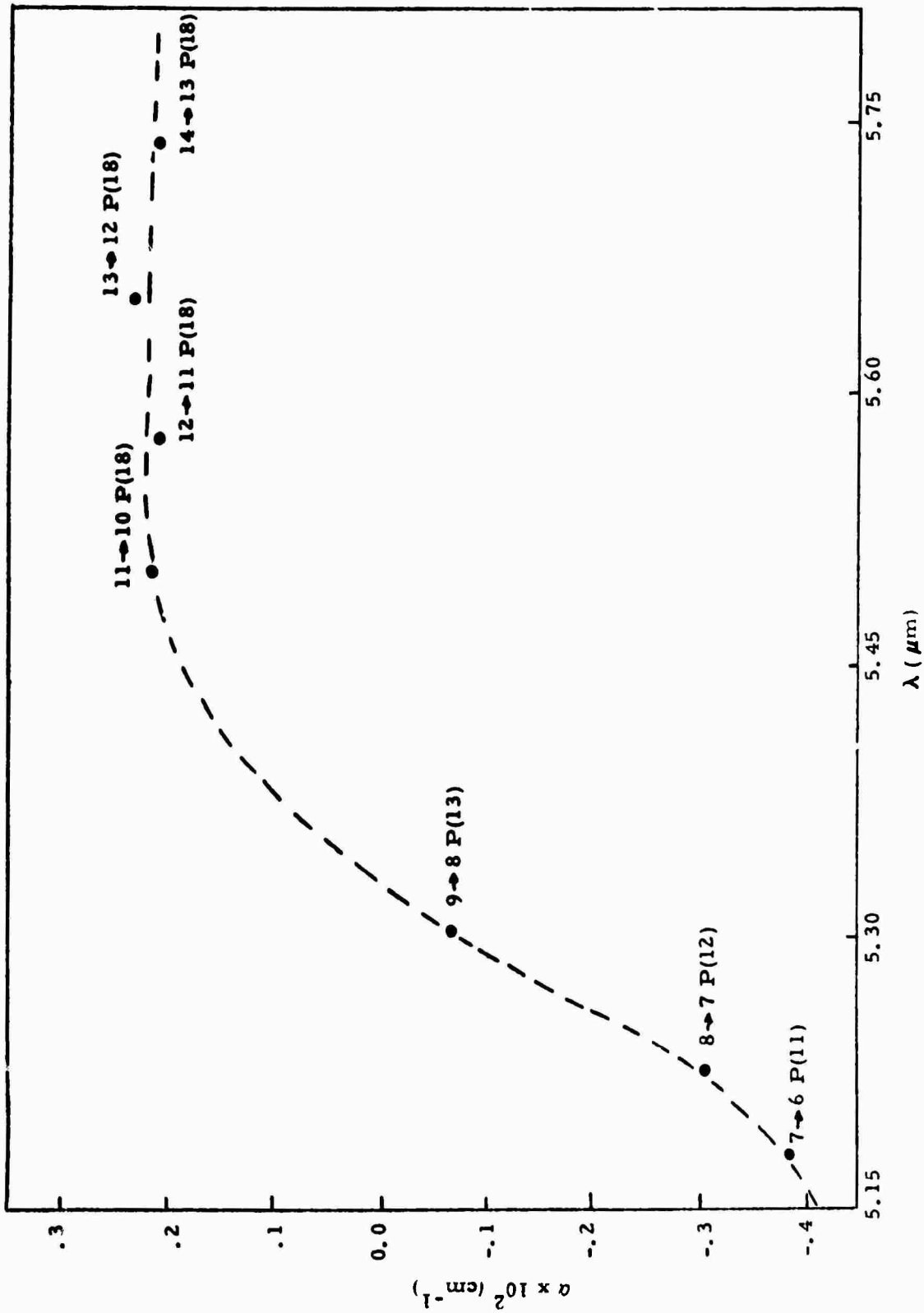


Figure 7.3 CO Laser Small Signal-Gains at 20°C Wall Temperature

used, since in this case the Doppler broadening was about three times larger than the collision broadening. Also, the rotational levels are assumed to be in a Boltzmann equilibrium at the gas temperature T.

The small signal gains were measured for 18 vibrational-rotational lines, and are given in Table IV. These values were fitted numerically to the above equation by a least square fitting method. The gas temperature that gave the best fit was found to be 124°K. The calculated values of α obtained by this method are shown in Table IV along with the measured values. The calculated population densities are given in Table V. A semilog plot of the population density versus the energy of the vibrational level, presented in Figure 7.4, shows the non-Boltzmann distribution at the levels where the population is inverted. The vibrational temperature between the levels shown in the Figure ($v = 5$ to 10) varies from 7270°K to 15,000°K.

The total number of CO molecules /cm³ at a CO partial pressure of 0.18 torr and 124°K is 1.5×10^{16} . The population density in the levels $v = 10$ to $v = 5$, where lasing occurs at this temperature, is $\sim 10^{15}$. Therefore, 6% of the total population density is found in the lasing levels, and this is of the same order of magnitude as that for the CO₂ laser.

The experimentally determined population given above also agrees rather well with the theoretical modeling computation for the same gas mixtures, presented in the companion report¹.

7.3 Measurement of Saturation Parameters. The saturation parameter of a high power laser like CO has a very important significance for systems application, since the product of the small signal gain and the saturation parameter represents the maximum power per unit volume

TABLE IV. CO LASER SMALL SIGNAL GAIN COEFFICIENT AT 124⁰K

BRANCH	J	MEAS GAIN	CALC GAIN	(MEAS-CALC)/MEAS
6 → 5	11	.0054	.00548172	- .01301623
	13	.0050	.00482665	.03467032
7 → 6	9	.0094	.00907838	.02955250
	10	.0101	.01012887	- .00478412
	11	.0096	.00956609	.00067797
	12	.0076	.00806507	- .05827430
	13	.0060	.00622002	- .04227372
	14	.0041	.00444748	- .08134773
8 → 7	9	.0121	.01261177	- .03841937
	10	.0129	.01239305	.03652783
	11	.0113	.01092629	.03568716
	12	.0086	.00883272	- .02360438
	13	.0065	.00662832	- .01974223
	14	.0044	.00465339	- .06855719
9 → 8	9	.0140	.01485677	- .05875831
	10	.0144	.01385291	.04035740
	11	.0125	.01182635	.05389170
10 → 9	9	.0137	.01370968	- .00006700

TABLE V. CO LASER POPULATION DENSITY

$$P_{\text{CO}} = 0.18 \pm 0.01 \text{ torr}$$

$$P_{\text{Total}} = 13.5 \text{ torr}$$

TEMP = 124°K

v	$N_v \text{ (cm}^{-3}\text{)}$
5	2.849×10^{14}
6	1.922×10^{14}
7	1.434×10^{14}
8	1.132×10^{14}
9	9.349×10^{14}
10	7.748×10^{13}

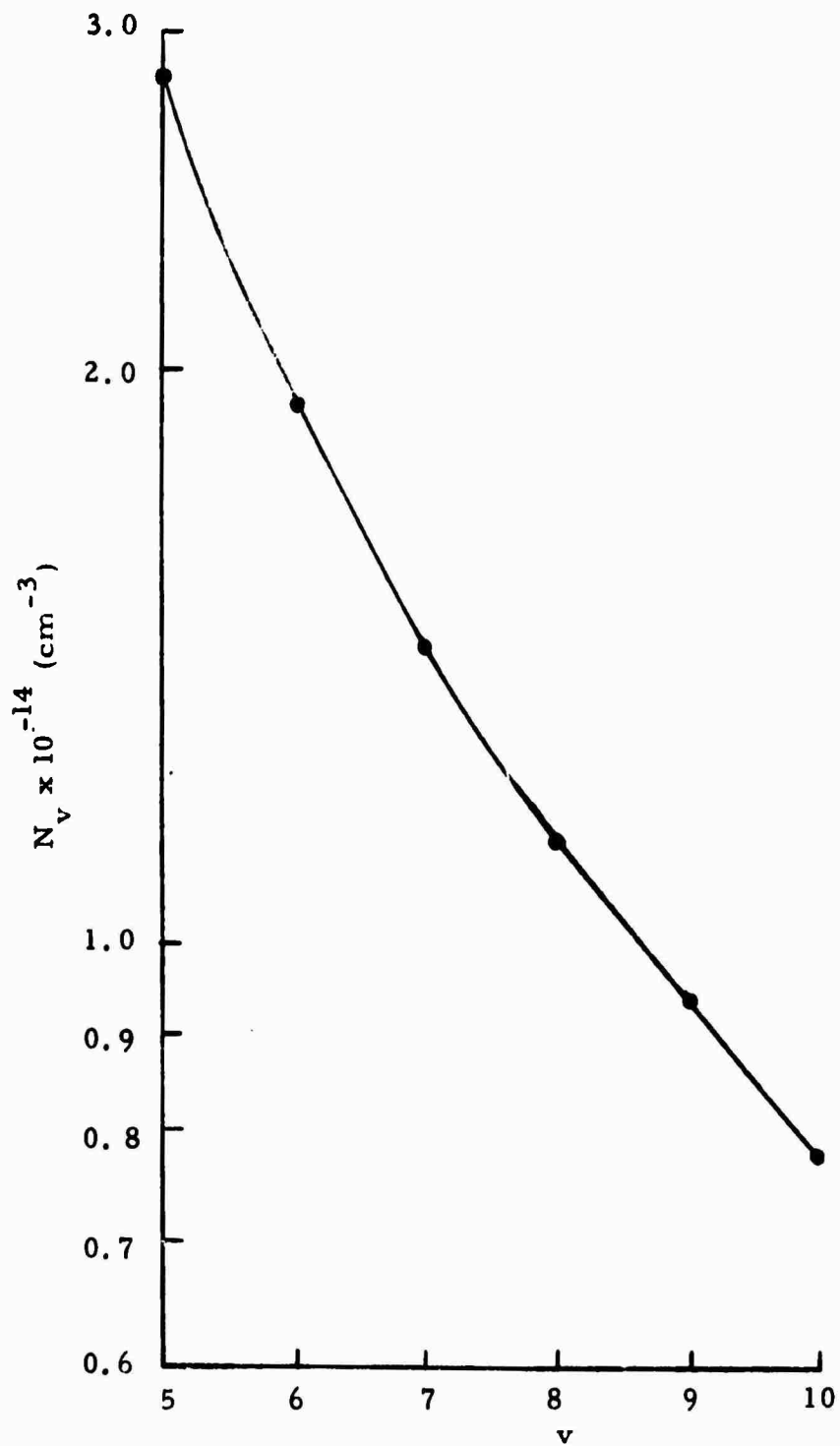


Figure 7.4 Populations of the various vibrational levels in a CO laser showing the non-Boltzmann distribution.

available for extraction. Therefore, estimates of the saturation parameter were obtained experimentally from the measurement of gain as a function of input intensities. The saturated gain for an inhomogeneously broadened line, as in the present case, is given by¹²

$$\alpha_I = \frac{\alpha_0}{\sqrt{1 + I/I_s}}$$

where α_I is the gain at an intensity I and α_0 is the small signal gain coefficient; I_s is the saturation parameter. Accordingly, for $I = I_s$, $\alpha_I = 0.7 \alpha_0$. In other words, the saturation intensity for an inhomogeneously broadened line is the intensity at which the gain coefficient is 70% of the small signal gain coefficient.

The gain coefficient for the various input intensities was measured for multiline operation at 125^oK gas temperature using the setup shown in Figure 7.1, with the exception of replacing the grating by a total reflector. The spot size of the beam was calculated to be 5 mm. The input intensities were determined from the measured power and the calculated spot size. The results are shown in Figure 7.5. The saturation parameter for multiline operation is determined from these data to be 4w/cm².

At higher intensities, the laser energy is extracted over the entire Doppler line width and therefore, the behavior in that region is more like that of homogeneously broadened line where:

$$\alpha_I = \frac{\alpha_0}{1 + I/I_s} .$$

Since the power inside the laser cavity is considerably higher, an estimate of the saturation parameter at higher intensities can be made by measuring the laser output power with different output coupling.

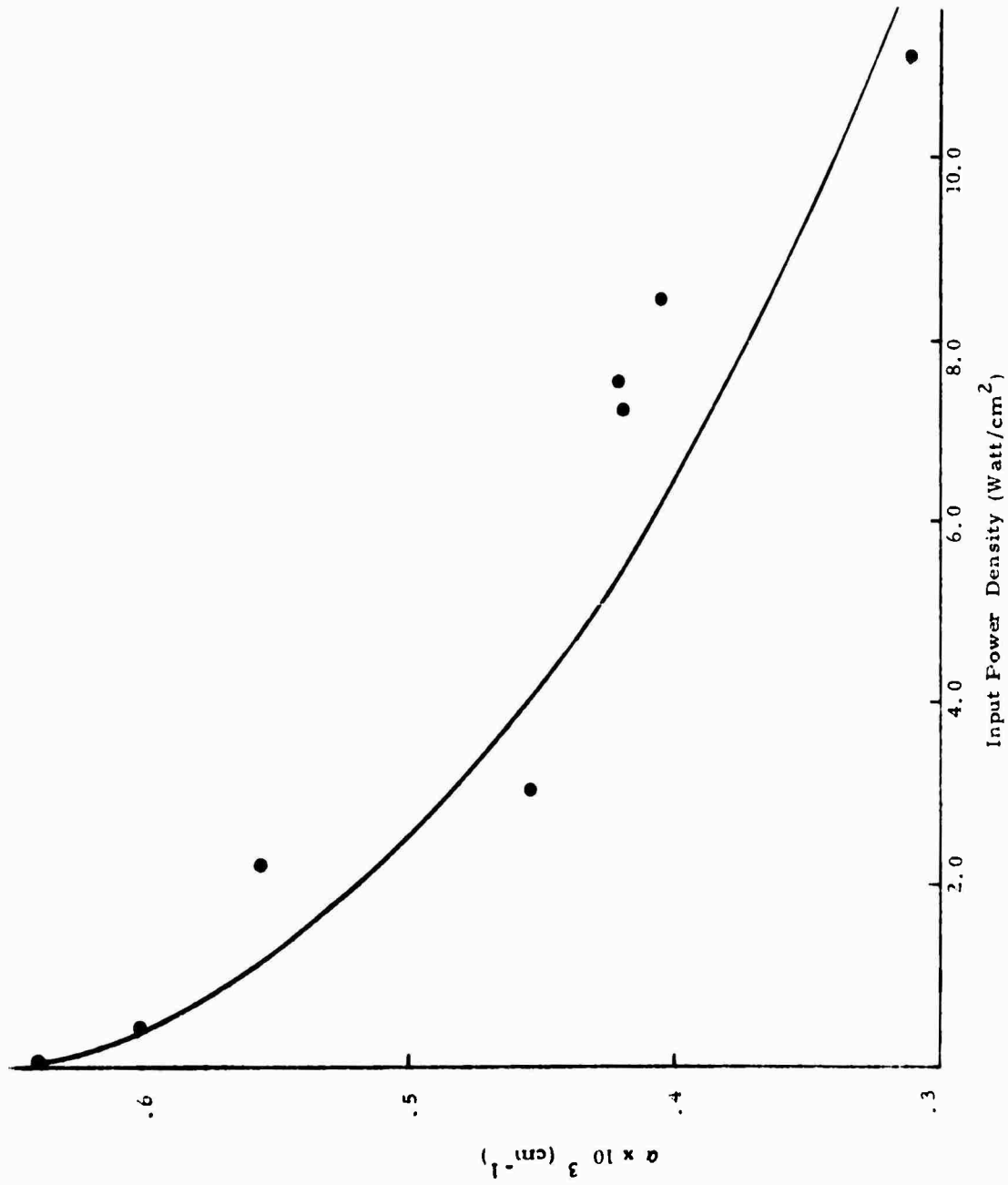


Figure 7.5 Saturated Gain vs. Input Power Density

An experiment was performed in which the 10 meter total reflector was left unchanged while the laser output power was measured with plane mirrors of different reflectivity. Under these conditions, the gain in two passes equals the mirror transmission loss. The intracavity power was simply the ratio of the output power to the mirror transmission coefficient. The gas temperature was estimated to be about 200^oK. The results of the experiment are given in Figure 7.6, where the gain coefficient is plotted as a function of cavity power. Since the multiline small signal gain coefficient at 124^oK was measured to be 0.064 per cm, the corresponding value at 200^oK determined from extrapolation of the curve in Figure 7.6 to be 0.045/cm, seems reasonable. The value of I_s at higher intensities is then determined to be 22 w/cm² at 200^oK.

The saturation parameter I_s is given by the expression $I_s = h\nu / \tau\sigma$ where τ is the inversion recovery time and σ is the stimulated emission cross-section. Since both τ and σ decrease with increasing temperature, the larger value of 22 w/cm² at 200^oK compared to 4 w/cm² at 125^oK is understandable.

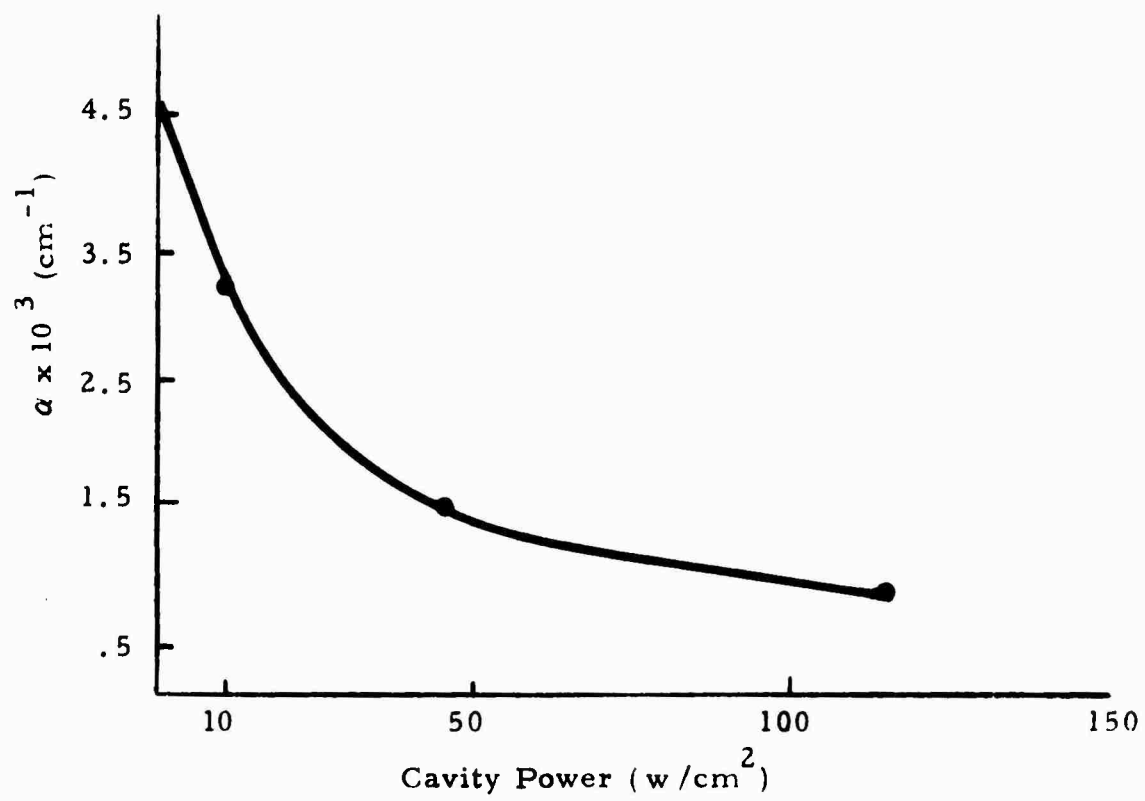


Figure 7.6 Gain vs. Cavity Power at High Powers

8.0 MEASUREMENT OF V-V RELAXATION RATE

It is evident from the discussion in the previous sections that the rates of vibrational cross-relaxation play a dominant role in controlling the molecular kinetics giving rise to population inversion. Therefore, an accurate value of the parameters is essential to the proper understanding of the CO laser mechanism. These parameters may be grouped into two types: (1) The rate of overall vibrational cross-relaxation, and (2) the rate of relaxation between individual vibrational levels.

The overall rate determines the characteristic time necessary to restore the equilibrium of all vibrational levels after the equilibrium has been disturbed in one or more levels by a process like lasing. In a CO laser this relaxation rate can be conveniently obtained by measuring the inversion recovery time in a Q-switching experiment. In fact, such experiments have been performed by Osgood et al¹⁴ and Yardley⁷. Osgood et al obtained the relaxation time from a double Q-switching experiment to be 70 μ sec. torr. Yardley obtained 208 μ sec. torr from a time resolved fluorescence measurement following Q-switching. Because of this disagreement in these reported rates, we have repeated the double Q-switching experiment. The details of the experiment are described below.

The laser tube was similar to that described in Section 4. The first Q-switched pulse was obtained from a cavity formed by a 10 meter mirror with 90% reflectivity, and a totally reflective rotating plane mirror. The second pulse was obtained by placing a second totally reflective stationary mirror facing the rotating mirror and at an angle of 10° with respect to the cooled laser tube. A gas mixture consisting of 15 torr He, .02 torr O₂, and 0.2 to 3.5 torr CO was used with a discharge current of 10 mA. The pulses were detected by a Ge: Au detector. Measurements were taken at sufficiently large pulse heights so that the Q-switched pulse in each case may be taken to be proportional to the population inversion.

The laser recovery time τ is given by

$$I_2 = I_1 (1 - e^{-t/\tau})$$

where I_1 is the height of the first pulse and I_2 is the height of the second pulse at a delay time t from the first pulse. Therefore the slope of a plot of $\ln(1 - \frac{I_2}{I_1})$ vs. t should give τ . The recovery time for a CO partial pressure of 3.5 torr is determined from Figure 8.1 to be 145 μ sec. This gives a value of 511 μ sec.torr which is in closer agreement with the value given by Yardley.

As indicated by Yardley⁷, the inversion recovery time provides the relaxation rate for different vibrational levels to a first approximation, since the relaxation of the near resonant vibrational levels of the CO molecules may be approximated by an ensemble of harmonic oscillators. According to this approximation, the relaxation time τ_{10} of the process $\text{CO}(v=1) + \text{CO}(v=0) \rightarrow \text{CO}(v=0) + \text{CO}(v=1)$ is twice as much as the overall relaxation time; i. e., the inversion recovery time and the relaxation time τ_{mn} for the process $\text{CO}(v=n) + \text{CO}(v=m) \rightarrow \text{CO}(v=n+1) + \text{CO}(v=m-1)$ is given by $\tau_{mn} = \tau_{10} / (n+1)m$.

Theoretical calculations¹⁵ predict that τ_{10} at the low temperatures is $\sim 10 \mu$ sec. According to the above discussions, the calculated value of τ_{10} would indicate a recovery time of 5 μ sec. The measured values are nearly two orders of magnitude longer. This discrepancy is probably due to the fact that the exact value of the relaxation rates between individual vibrational levels are quite different than the value given by the above formula. This difference may be expected due to the deviation from exact resonance in vibrational energy of the various levels as a result of the anharmonicity of the CO molecules. Experiments are now being planned to determine more accurate values of the relaxation rates between individual levels.

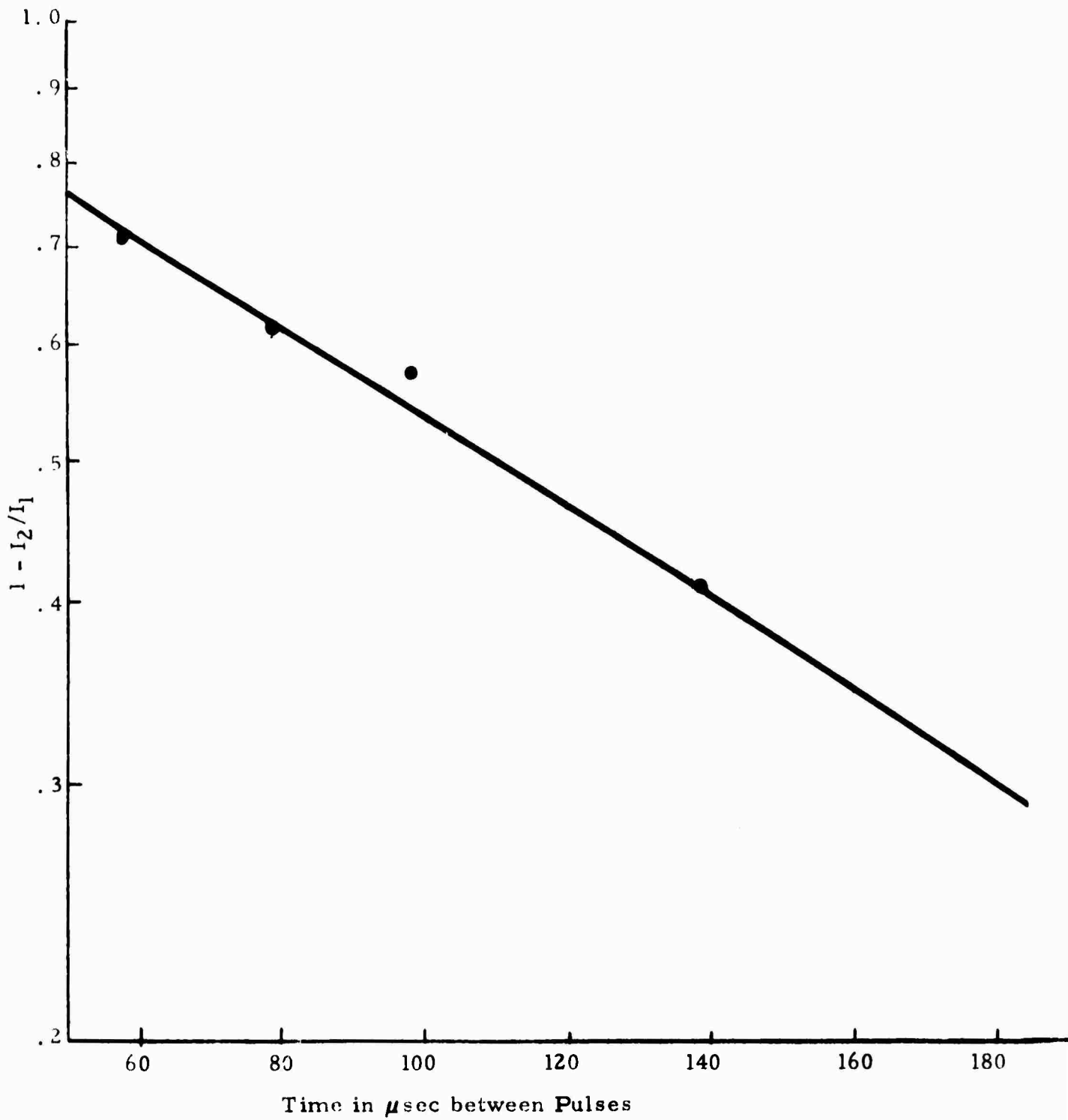


Figure 8.1 Results of Double Pulsed Q-Switching Experiment

9.0 CONCLUSION

The results of the investigations reported in Section 4 through Section 8 support the discussion on the mechanisms of the CO laser given in Section 3. In brief, the study shows that the population inversion in a CO laser occurs by vibrational excitation to the lower vibrational levels by electron impact, followed by anharmonic pumping of the molecules to the lasing levels.

The role of various gas constituents discussed in Section 5 clearly indicates the importance of controlling average electron energy for efficient pumping of the electrical energy into vibrational excitation. Since the efficiency is generally increased by lowering the electron temperature for better coincidence with the electron excitation cross-section, the primary pumping process should be due to electronic impact excitation of the vibrational levels. The vibration population in lasing levels ($v = 10$ to $v = 5$) is found to be about 6%; therefore most of the population is in the lower levels including the ground state. Thus the primary excitation must proceed through vibrational excitation of the lower levels.

The preponderance of anharmonic pumping, in bringing about partial population inversions in the higher vibrational levels is clearly demonstrated by the spectral study presented in Section 6. Finally, the close agreement of the measured population densities given in Section 7 with those predicted by theoretical modeling based on the mechanisms described above leave little doubt about the validity of the mechanisms.

The operating characteristics of the CO laser, with respect to small signal gain and saturation parameters, are found to be quite similar to those for the CO₂ laser, even though the mechanisms of population

inversion are significantly different in the two cases. The primary difference, of course, is the high efficiency that is achievable with the CO laser. The attainment of 47% is by no means the ultimate to be expected from a CO device; by proper utilization and optimization of plasma characteristics, it should be possible to improve the fractional transfer of electrical to vibrational energy. Nighan⁹ has shown that, for proper values of E/N, almost 100% of the electrical energy in a glow discharge can be put into levels 1 to 8 of the CO molecule.

Of course, several factors have been neglected in this prediction. For example, VV pumping involves a concomitant heating of the gas, because of the anharmonic defect of the CO molecules and therefore must involve the transfer of small percentage of energy to or from kinetic energy for every VV collision that is not exactly resonant. There will also be heating due to VT relaxation processes, although VT rates are small for the lower levels of CO. These two effects must be taken into account for the determination of the theoretical "quantum efficiency" that is attainable for a CO laser under a given set of operating conditions. Furthermore, there will be other mechanisms, such as heating in the cathode fall region, as well as heating by ion collisions, which will act to limit the actual efficiency that can be realized for a given system. It is not unreasonable, however, to expect overall efficiencies much greater than 50% for optimum configurations of an electrical discharge CO laser system.

10. REFERENCES

1. W. B. Lacina, "Kinetic Model and Theoretical Calculations for Steady State Analysis of Electrically Excited CO Laser Amplifier System," NCL Report 71-32R, Aug. 5, 1971.
2. R. C. Millikan and D. R. White, "Systematics of Vibrational Relaxation," J. Chem. Phys., Vol. 39, Dec. 15, 1963, pp 3209-3213.
3. R. C. Millikan, "Vibrational Fluorescence of Carbon Monoxide," J. Chem. Phys., Vol. 38, June 15, 1963, pp 2855-2860.
4. D. J. Miller and R. C. Millikan, "Vibrational Relaxation of Carbon Monoxide by Hydrogen and Helium Down to 100^oK," J. Chem. Phys. (Letters), Vol. 53, 1970, pp 3384-3385.
5. C. E. Treanor, J. W. Rich, and R. G. Rehm, "Vibrational Relaxation of Anharmonic Oscillators with Exchange-Dominated Collisions," J. Chem. Phys., Vol. 48, Feb. 15, 1968, pp 1798-1807.
6. G. J. Schulz, "Vibrational Excitation of N₂, CO, and H₂ by Electron Impact," Phys. Rev., Vol. 135A, Aug. 17, 1964, pp 988-994.
7. J. T. Yardley, "Vibrational Energy Transfer in CO-He Lasers," J. Chem. Phys., Vol. 52, April 15, 1970, pp 3983-3989.
8. W. L. Nighan, W. J. Wiegand, M. C. Fowler, and R. H. Bullis, "Investigation of Plasma Properties of High Energy Gas Discharge Lasers," United Aircraft Report, 1970.
9. W. L. Nighan and J. H. Bennett, "Electron Energy Distribution Functions and Vibrational Excitation Rates in CO₂ Laser Mixtures," Appl. Phys. Lett., Vol. 14, April 15, 1969, pp 240-243.

10. W. L. Nighan, "Electron Energy Distributions and Collision Rates in Electrically Excited N₂, CO, and CO₂," *Phys. Rev.*, Vol. 2A, Nov., 1970, pp 1989-2000.
11. R. M. Osgood, W. C. Eppers, and E. R. Nichols, *IEEE, J. Q. E.*, Vol. 6, 145, 1970.
12. B. F. Gordietz, N. N. Sobolev, V. V. Sokovikov, and L. A. Shelepin, *IEEE; J. Q. E.* Vol. 4, 796, 1968.
13. A. Yariv, "Quantum Electronics," John Wiley and Sons, pp 267.
14. R. M. Osgood, E. R. Nichols, and W. C. Eppers, *Appl. Phys. Letters*, Vol. 15, 1969, pp 69.
15. W. Q. Jeffers and J. D. Kelley, (Private communication).